forests

MDPI

Article

Vegetation Dynamics since the Last Glacial Maximum in Central Yunnan, Southwest China

Min Wang [1], Caiming Shen [1,*], Qifa Sun [2,*], Hongwei Meng [1], Linpei Huang [1], Hucai Zhang [3] and Huiling Sun [1]

[1] Yunnan Key Laboratory of Plateau Geographical Processes and Environmental Changes, Faculty of Geography, Yunnan Normal University, Kunming 650500, China; wang_min@ynnu.edu.cn (M.W.); menghw@ynnu.edu.cn (H.M.); linpei_huang@ynnu.edu.cn (L.H.); sunhuiling@ynnu.edu.cn (H.S.)
[2] College of Resources, Environment and Chemistry, Chuxiong Normal University, Chuxiong 675000, China
[3] Institute for Ecological Research and Pollution Control of Plateau Lakes, School of Ecology and Environmental Science, Yunnan University, Kunming 650500, China; zhanghc@ynu.edu.cn
* Correspondence: caiming_shen@ynnu.edu.cn (C.S.); sunqifa@cxtc.edu.cn (Q.S.)

Abstract: Vegetation dynamics data since the Last Glacial Maximum (LGM) are essential for our understanding of ecosystem shifts and vegetation responses to climate change. Here, we present a pollen record covering the last 25,000 years from Lake Fuxian in central Yunnan, southwest China. Our study shows seven stages of vegetation dynamics since the LGM: The early LGM (stage 7 of 25,000–21,200 cal. a BP) witnessed less dense regional vegetation dominated by pine forests, evergreen broadleaved forests (EBFs), deciduous broadleaved forests (DBFs), montane hemlock forests, and fir/spruce forests. The late LGM (stage 6 of 21,200–17,500 cal. a BP) saw an expansion of grasslands, wetlands, and montane fir/spruce forests as well as a shrinkage of EBFs and DBFs. During the last deglaciation (stage 5 of 17,500–13,300 cal. a BP), dense regional vegetation was dominated by EBFs as well as deciduous oak and alder forests. The densest regional vegetation occurred in stage 4 of 13,300–11,200 cal. a BP, roughly equal to the Younger Dryas Chron, when pine forests, DBFs, EBFs, grasslands, and wetlands grew in the Lake Fuxian catchment. During the early to mid-Holocene (stage 3 of 11,200–5000 cal. a BP), dense regional vegetation was dominated by sweetgum forests, in addition to some pine forests and EBFs. After 5000 cal. a BP, the regional vegetation density became lower and lower, and forests became thinner and thinner. Pine forests expanded to their maximum of the entire sequence in stage 2 of 5000–2500 cal. a BP. A big deforestation event occurred in stage 1 (the last 2500 years), when grasslands, wetlands, and cultivated vegetation dominated regional vegetation in the catchment of Lake Fuxian. The regional vegetation since the LGM in the catchment of Lake Fuxian also experienced six major transitions, five centennial shift events, and one big large-scale and long-term deforestation event. These resulted from the responses of regional vegetation to climate changes during the LGM, last deglaciation, and early–mid-Holocene, as well as human influence in the late Holocene. The vegetation density since the LGM has changed with the 25° N summer insolation.

Keywords: fossil pollen; plant abundance; forest; vegetation density; large lake; Yunnan

Citation: Wang, M.; Shen, C.; Sun, Q.; Meng, H.; Huang, L.; Zhang, H.; Sun, H. Vegetation Dynamics since the Last Glacial Maximum in Central Yunnan, Southwest China. *Forests* **2024**, *15*, 1075. https://doi.org/10.3390/f15071075

Academic Editor: Phillip G. Comeau

Received: 12 May 2024
Revised: 11 June 2024
Accepted: 18 June 2024
Published: 21 June 2024

1. Introduction

Yunnan lies at the southeastern edge of the Tibetan Plateau. It is a low-latitude plateau. Its elevation falls step by step from its northwest of about 3000–4000 m above sea level (a.s.l.), to its middle of about 2000–2500 m a.s.l., and to its south of about 1200–1500 m a.s.l. [1]. It is divided into the west valleys and the east plateau by the Diancang Mountains and Ailao Mountains. In northwest Yunnan, the Hengduan Mountains stretch from north to south, and the Mountains Gaoligongshan, Nushan, and Yunshan are situated from west to east, separated by Rivers Nujiang, Lancangjiang, and Jinshajiang. In east Yunnan, the diverse mountainous basins and fault lakes developed in hilly terrains with a lot of karst landforms. In south and southwest Yunnan, landforms with crisscross

mountains, hills, and basins have developed [2]. The exceptionally varied topography and great elevation differences in Yunnan, with the highest elevation of 6740 m a.s.l. and the lowest elevation of 76.4 m a.s.l., cause huge climatic gradients, with the mean annual temperature (MAT) varying from above 24 °C to below 5 °C, and the mean annual precipitation (MAP) varying from above 4000 mm to below 300 mm [3], thus resulting in a variety of vegetation types. The vegetation, occupying the Yunnan Plateau, includes tropical rainforests, subtropical EBFs (the vast majority), warm–temperate DBFs, temperate coniferous and broadleaved mixed forests, cold–temperate coniferous forests, alpine scrub communities, meadows, and wetlands, as well as thorny shrublands and savannas in hot–dry valleys [4]. Yunnan, as a plant kingdom and a biodiversity hotspot [5], offers a natural laboratory for understanding the short-term responses and interactions between forests and environments. It is evident that paleoecological studies are needed to understand the long-term dynamics of the vegetation. This issue attracted international attention as early as in 1981, at the start of a Sino–Australian Quaternary collaborative project [6] which involved the pollen analysis of lacustrine deposits in Yunnan [7–10]. Since then, pollen analysis, an effective technique to study past vegetation [11], has extensively been used in the studies of Quaternary vegetation histories in Yunnan (e.g., [12–19]). However, few of those studies focused on the time periods longer than the Holocene due to the scarcity of natural archives and difficulties in obtaining them. After 26,000 cal. a BP (before present; "present" refers to 1950 A.D.), the earth experienced the cold conditions of the LGM (26,000–19,000 cal. a BP) [20], a quick warming from the last deglaciation [21], and warm conditions of the current interglacial period (the Holocene) [22], as well as cold/warm conditions of stadials/interstadials [23] and a series of centennial–millennial climatic events [24] in the glacial and interglacial periods. Knowledge on vegetation composition and dynamics in space and time is still very limited in Yunnan, and even globally, to quantify or predict the future emergence of new ecosystems caused by glacial retreat [25] and to answer the deglacial forest conundrum [26] and Holocene temperature conundrum [27]. Although some long pollen records since the LGM are available for the Lakes Lugu [28], Shudu [29], Wenhai [30], and Qinghai [31] in northwestern Yunnan, and Lakes Dianchi [32], Xingyun [33], and Yilong [34] in central–southern Yunnan, more records are essential so that we can understand the temporal and spatial patterns of vegetation dynamics since the LGM and their possible mechanisms in Yunnan, and even southwest China.

The REVEALS (Regional Estimates of VEgetation Abundance from Large Sites) model is a validated approach for estimating regional vegetation abundance using fossil pollen counts, applicable to fossil pollen records from lakes and swamps [35–37]. Pollen records from large lakes will offer us an opportunity to use the plant abundance (PA) estimated using the REVEALS model to interpret regional vegetational dynamics and to examine its applications in pollen records of large lakes.

In this study, we present a fossil pollen record of a core from Lake Fuxian, a large and deep lake in central Yunnan [38]. The pollen percentage, pollen influx, and PA were used to reveal the forest dynamics since the LGM as well as their responses to climatic and anthropogenic forcings.

2. Site Description

Lake Fuxian (24°21′–24°38′ N, 102°49′–102°58′ E, 1721 m a.s.l.) (Figure 1a) is located in the Chenjiang basin of central Yunnan. It is a large and deep lake, formed by a fault depression during the Tertiary uplift in the Yunnan Plateau [39,40]. Its water area, average and maximum water depths, and catchment area are 212 km^2, 89.6 and 155 m, and 674.7 km^2 (Figure 1b) [40]. It is the deepest lake in the Yunnan Plateau. Its catchment is part of the Nanpanjiang system in the Pearl River Basin [41]. The replenishment of the lake water mainly depends on rainfall and surface runoffs. More than 20 mountain streams, such as the Jianshan, East, and West Rivers, flow into the lake. Its water outlet is the Haikou River in the east of the lake, which flows into the Nanpanjiang River [40].

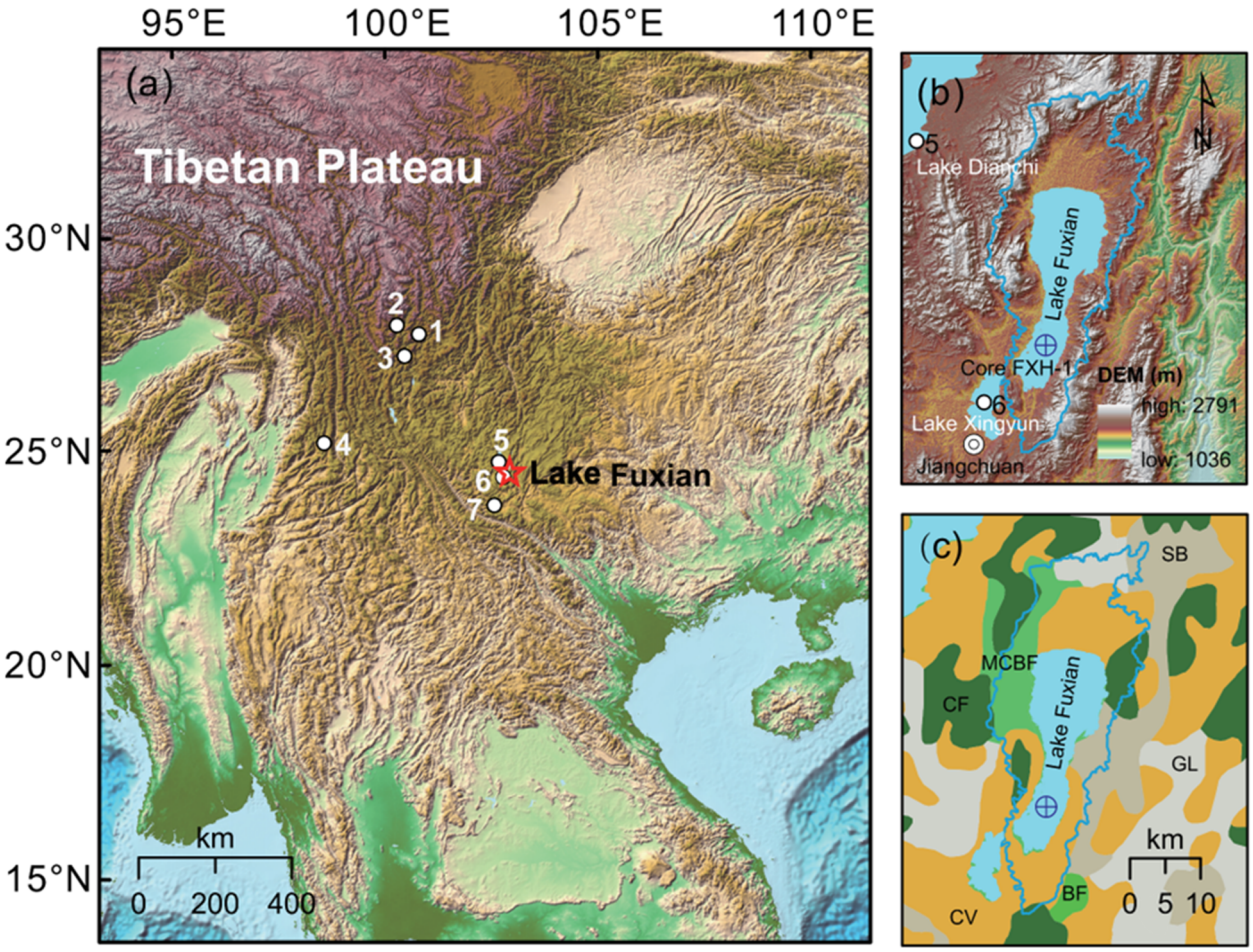

Figure 1. Location, topography, and vegetation of Lake Fuxian, the study site. (**a**) Topographic map showing the locations of Lake Fuxian and the lakes mentioned in this study (1–4 represent Lakes Lugu, Shudu, Wenhai, and Qinghai in northwestern Yunnan, 5–7 represent Lakes Dianchi, Xingyun, and Yilong in central and southern Yunnan); (**b**) topography of the Lake Fuxian catchment (the area bounded by blue lines) and location of the study core (dark blue cross in circle); (**c**) modern vegetation in the Lake Fuxian catchment [42] (CF = coniferous forest, BF = broadleaved forest, MCBF = mixed coniferous and broadleaved forest, SB = scrub, GL = grassland, and CV = cultivated vegetation).

Geomorphologically, Lake Fuxian, in the center of the lake catchment, has straight lake shorelines (Figure 1b). The lake is aligned north–south, with two large ends and one narrow middle. The lake basin and banks exhibit the characteristics of a typical graben rift lake. The Lake Fuxian basin is surrounded by mountains, most of which are eroded fault-block mountains of about 2500 m a.s.l., with the west higher than the east and the north higher than the south, extending from south to north. The higher peaks include Mounts Gudui, Sanlingzi, Sanliangzi, and Bizi, with elevations of 2500–2650 m. The northern and southern ends of the lake are lacustrine–alluvial plains with gentle shore zones. The northern plain covers a large area, about 40 km^2, sloping from north to south and containing many ponds and marshes due to the undulating terrain. The southern plain is smaller. On the east and west sides of the lake, the terrain is steep, and the cliffs edge to the lake, forming steep, rocky bank belts. The east and west banks are surrounded by middle and low mountains [43].

Climatologically, the Lake Fuxian catchment has a semi-humid subtropical monsoon climate, controlled by westerlies in the winter-half of the year and monsoons in the summer-half of the year. The climatic data of 1960–2019 (Figure 2) from Jiangchuan meteorological station (24°17′ N, 102°46′ E, 1731 m) show a 60-a MAP, MAT, and mean annual humidity

(MAH) of 850 mm, 16.0 °C, and 70.8%, respectively. Regarding the annual precipitation, 716 mm (over 83%) is concentrated in the rainy season from May to October, mostly brought about by the South Asian summer monsoon. The climate of the Lake Fuxian catchment exhibits obvious wet and dry seasons, with a warm–dry spring, not-hot summer, cool and less rainy autumn, and mild winter (Figure 2) [39].

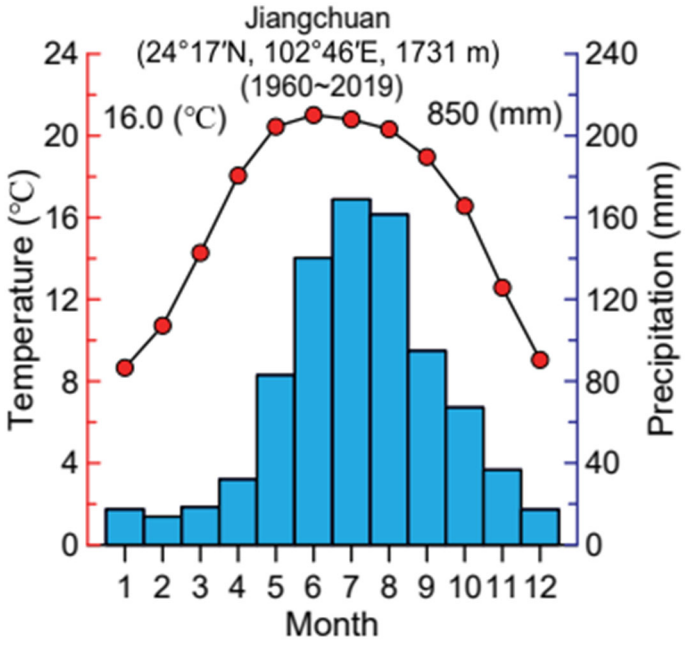

Figure 2. The 1960–2019 monthly mean precipitation and temperature at Jiangchuan meteorological station, the closest station to Lake Fuxian.

Phytogeographically, the terrains of the lake catchment are today occupied by native and artificial vegetation (Figure 1c). The native vegetation includes coniferous forests, EBFs, DBFs, scrubs, and grasslands [2]. The artificial vegetation includes economic forests and crops in paddy fields and drylands. The forests, accounting for 47% of the lake basin's land area, are composed of *Pinus yunnanensis*, *P. armandi*, *Castanopsis delavayi*, *Cyclobalanopsis delavayi*, *C. glaucoides*, *Quercus acutissima*, *Q. variabilis*, and *Alnus nepalensis* [44]. Among them, *Pinus yunnanensis* forests make up the majority of existing forests (ca. 70%), growing in the hilly terrains at 1500–2800 a.s.l. Its tree layer is dominated by *Pinus yunnanensis*, often along with *Castanopsis delavayi*, *Keteleeria evelyniana*, *Alnus nepalensis*, and *Cyclobalanopsis delavayi*; its shrub layer consists mainly of species of Ericaceae and Rosaceae [2,44]. Broadleaved forests, ca. 30% of the existing forests, involve EBFs such as *Lithocarpus variolosus*, *Cyclobalanopsis glaucoides*, *C. delavayi*, and *Castanopsis delavayi* and DBFs such as *Quercus acutissima*, *Q. variabilis*, and *Alnus nepalensis* [45].

3. Materials and Methods

In 2013, a 906 cm sediment core (core FXH-1) was taken from the center of southern Lake Fuxian (24°25′24″ N, 102°52′24″ E, 1721 m a.s.l.) under 81.2 m of water (Figure 1b) using the above-water platform and the Austrian UWITEC piston sampling equipment. Nine bulk organic samples from this core were sent to the Beta Laboratory in the United States for AMS ^{14}C dating.

The core was sampled for pollen analysis at 1–10 cm irregular intervals. A total of 96 pollen samples (each 0.5–1 g) were treated with a standard method, in which HCl (10%), KOH (10%), HF (40%), and acetolysis were involved [46]. Tablets with a known number of *Lycopodium* spores were added to the samples as a marker to determine the pollen concentrations and influx values [47]. The pollen influx was calculated using the pollen concentrations and sedimentary rates, i.e., pollen concentration (grains/cm^3) ×

sedimentary rate (cm/a). The sedimentary rates were derived from the age–depth model of the studied core. The total pollen influx values in this study were used as a proxy of the vegetation density [48]. The identification and counting of pollen were conducted under an Olympus optical microscope (made by Olympus Corporation, Tokyo, Japan) with a magnification of 400 times. More than 500 terrestrial pollen grains were counted for each sample. The pollen percentage was calculated using the sum of terrestrial plant pollen. The pollen percentage and influx diagrams of major pollen taxa were plotted using TILIA software (version 3.0.1) (Minneapolis, IL, USA) [49].

In this study, fossil pollen spectra were divided into 7 pollen zones in terms of the cluster analysis result of the main pollen percentages [50]. A PCA (principal component analysis) of the main pollen percentage data was performed to assist the vegetational interpretation of fossil pollen spectra and zones. The PCA was conducted in the "factoextra" package (version 1.0.7) [51] within R software (version 4.3.2) (Vienna, Austria) [52]. The REVEALS model was used in the estimation of the past PA of the RVC (regional vegetation composition) in terms of pollen counts [36]. In this procedure, Poaceae was chosen as the reference taxon, and the pollen fall rates for various pollen taxa in the study region were estimated [53]; the relative pollen production (RPP) and regional PA across different plant taxa were estimated via the "disqover" R package (version 0.9.09) [54] within R software.

4. Results

4.1. Stratigraphy and Chronology of Core FXH-1 from Lake Fuxian

The upper 0–832 cm part of the 906 cm core is studied here. This part is mainly composed of silty clays. Three lithological units can be recognized from the sediment color (Figure 3). The 0–140, 140–390, and 390–832 cm units contain brick-red, light grey, and dark grey silty clays with high, moderate, and low redness, respectively.

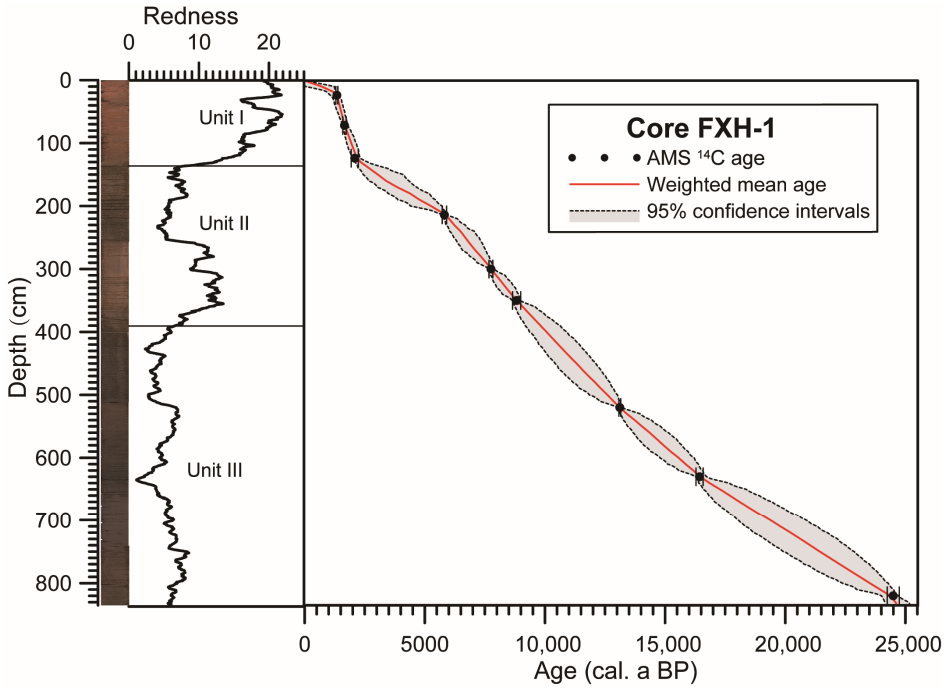

Figure 3. Lithology, redness, and age–depth model for core FXH-1 from Lake Fuxian.

No plant remains were found in core FXH-1, so the materials used for AMS ^{14}C dating are bulk organic matter. The dating results of nine bulk organic samples are shown in Table 1. The AMS ^{14}C dates at 3 cm from a core near core FXH-1 and modern submerged plants are 160 ± 30 and 106.7 ± 0.3 ^{14}C a BP [55], suggesting that Lake Fuxian has a very small or no reservoir effect, which is negligible. Therefore, the ^{14}C dates from bulk organic matter were not corrected for any reservoir age, and they were calibrated using

IntCal20 [56]. The sediment top age of core FXH-1 was set to −63 cal. a BP (2013 A.D., the coring year). This age and the nine ^{14}C dates were then used to develop the age–depth model of core FXH-1 from Lake Fuxian (Figure 3). The age–depth model shows that unit I (0–140 cm) has the highest, whereas unit III (360–832 cm) has the lowest sedimentary rates.

Table 1. AMS ^{14}C dating results for core FXH-1 from Lake Fuxian in central Yunnan, SW China.

Lab ID	Depth (cm)	Dating Material	^{14}C Age (a BP)	Calibrated Age/2σ (cal. a BP) *	Median Age (cal. a BP)
Beta-518737	24	Bulk organic	1460 ± 30	1390–1300	1340
Beta-518738	72	Bulk organic	1780 ± 30	1740–1590	1660
Beta-518739	124	Bulk organic	2120 ± 30	2290–2000	2080
Beta-518740	214	Bulk organic	5110 ± 30	5930–5750	5810
Beta-518741	300	Bulk organic	6930 ± 30	7840–7680	7750
Beta-518742	350	Bulk organic	7950 ± 30	8990–8650	8820
Beta-518743	520	Bulk organic	11,190 ± 30	13,170–13,090	13,110
Beta-518744	630	Bulk organic	13,610 ± 40	16,590–16,290	16,430
Beta-518745	820	Bulk organic	20,400 ± 60	24,740–24,230	24,490

* Calibrated using IntCal20 [56].

4.2. Pollen Record of Core FXH-1 from Lake Fuxian

Pollen spectra of core FXH-1 are predominated by arboreal pollen (AP), including coniferous pollen taxa as well as deciduous and evergreen broadleaved pollen taxa. Among coniferous pollen taxa, *Abies*/*Picea*, *Tsuga*, and *Pinus* are common taxa. Common evergreen broadleaved pollen taxa contain evergreen *Quercus* [*Quercus* (E)], *Cyclobananopsis*, and *Castanopsis*-type (mostly *Castanopsis*/*Lithocarpus*, rarely *Castanea*). Deciduous broadleaved tree pollen taxa mainly include deciduous *Quercus* [*Quercus* (D)], *Liquidambar*, *Pterocarya*, *Alnus*, *Ulmus*, and *Betula.* Herbaceous pollen types contain Poaceae, Labiatae, Cyperaceae, *Artemisia*, and Asteraceae. In terms of the result of the CONISS analysis on pollen percentage data of major pollen taxa, 96 pollen samples of core FXH-1 are chronologically classified into seven pollen zones (Figure 4):

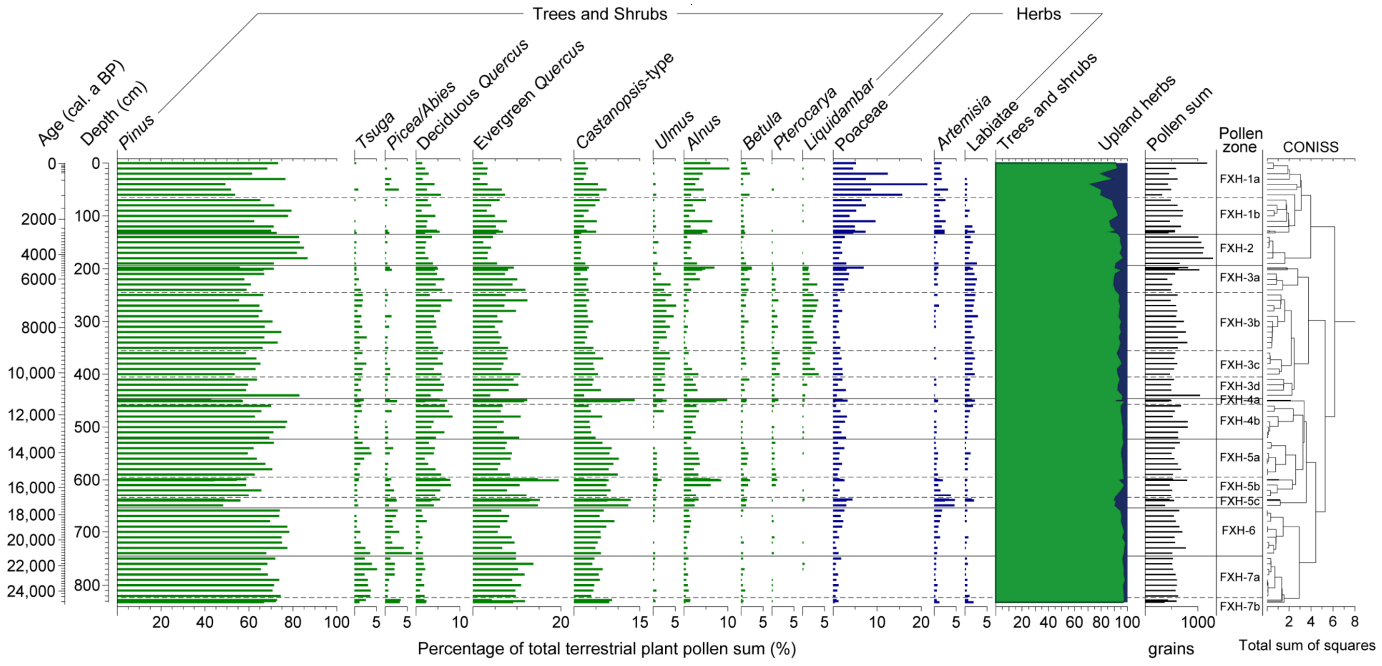

Figure 4. Pollen percentage diagram of main pollen taxa for core FXH-1 from Lake Fuxian.

Pollen zone FXH-7 (832–745 cm; 25,000–21,200 cal. a BP): This zone, consisting of 11 pollen spectra, is characterized by the highest AP and the lowest herbaceous pollen of the entire core (96.2–98.5/97.4% and 1.5–3.8/2.6%, the minimum–maximum/average of pollen spectra in the zone or subzone, the same as below). Among AP, *Pinus* is the most abundant pollen (65.3–74.4/70.5%), followed by *Quercus* (E) (4.2–13.7/10.0%), *Castanopsis*-type (3.9–8.6/5.5%), *Tsuga* (1.0–5.1/2.9%), Rosaceae (0.8–4.1/2.9%), *Quercus* (D) (0.9–2.4/1.7%), *Abies*/*Picea* (0–3.5/1.5%), and *Alnus* (0.3–1.4/0.8%) pollens. Poaceae (0.3–1.7/0.8%), Labiatae (0.2–1.9/0.6%), and *Artemisia* (0.2–1.1/0.5%) are common herbaceous pollen types. The pollen influx diagram (Figure 5) shows that total pollen influx values in this zone are low (1533–4399/2512 grains cm^{-2} a^{-1}). This zone can be further divided into two subzones. Subzone 7b (three fossil pollen spectra) is distinguished from subzone 7a (eight fossil pollen spectra) by a significant increase in *Castanopsis*-type and *Abies*/*Picea* pollens, as well as a rise of total pollen influx values.

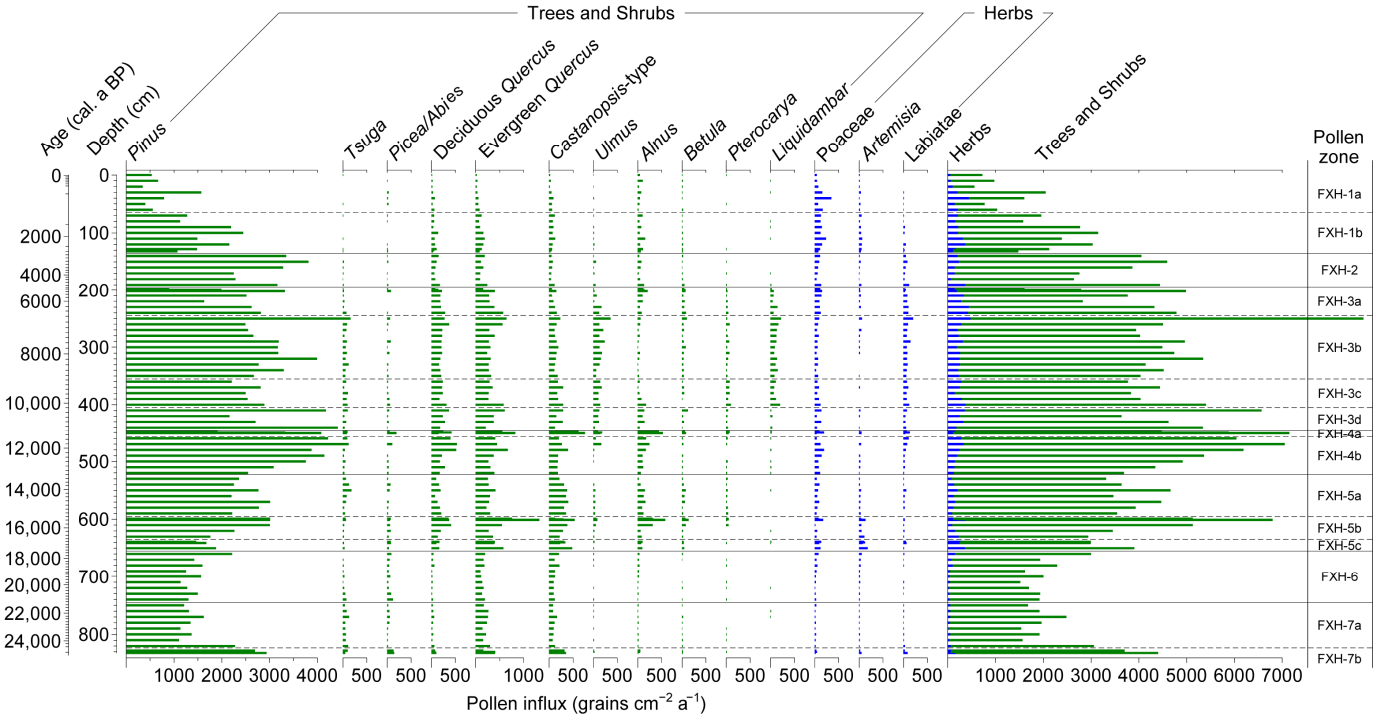

Figure 5. Pollen influx diagram of main pollen taxa for core FXH-1 from Lake Fuxian.

Pollen zone FXH-6 (745–655 cm; 21,200–17,500 cal. a BP): This zone, which consists of nine pollen spectra, is characterized by a rise in the pollen percentages of *Pinus* (67.8–78.3/74.2%) and *Picea*/*Abies* (1.3–6/2.7%). *Picea*/*Abies* increases to its maximum, and *Pinus* pollen increases to its second maximum in the core. *Tsuga* (0–3.5/1.2%), *Quercus* (E) (5.5–9.7/7.6%), *Quercus* (D) (0.5–2.4/1.2%), Rosaceae (0.3–1.9/1.0%), *Ulmus* (0–0.4/0.2%), and *Betula* (0–0.5/0.2%) pollens decrease. *Castanopsis*-type (4.8–9.2/6.3%), *Alnus* (0.4–1.6/1%), Poaceae (0.4–2.5/1.4%), and *Artemisia* (0.4–1.7/1%) pollens increase. The pollen influx values in this zone (1515–2996/1987 grains cm^{-2} a^{-1}) are slightly lower than those of zone FXH-7.

Pollen zone FXH-5 (655–525 cm; 17,500–13,300 cal. a BP): In this zone, consisting of 17 pollen spectra, the *Pinus* pollen percentages (44.3–71.2/58.8%) drop to its minimum of the entire core. *Picea*/*Abies* pollen (0–2.6/1.0%) declines too. The pollen percentages of *Quercus* (E) (5.6–19.5/10.7%), *Quercus* (D) (2.0–8.0/4.7%), *Castanopsis*-type (2.3–12.9/8.4%), *Alnus* (0.6–8.4/3.6%), *Betula* (0.3–2/1.1%), and *Pterocarya* (0–1.2/0.4%) increase. Herbaceous pollens such as Poaceae (0.2–4.3/1.9%), *Artemisia* (0.3–4.6/1.7%), and Labiatae (0–2.0/0.6%) increase slightly. The pollen influx values (2599–6796/3940 grains cm^{-2} a^{-1}) double

those of zone FXH-6. This zone can be further divided into three subzones. Subzone 5c is distinguished from the other two subzones by lower *Pinus* and higher *Quercus* (D), *Castanopsis*-type, Poaceae, and *Artemisia* pollens, as well as the lowest pollen influx values among the three subzones. Subzone 5a contains more *Tsuga* and *Castanopsis*-type and less *Quercus* (D) and *Quercus* (E) pollens than subzone 5b.

Pollen zone FXH-4 (525–446 cm; 13,300–11,200 cal. a BP): In this zone, which consists of 10 pollen spectra, *Pinus* (42.7–77.3/64.8%) and *Quercus* (D) (2–8.3/5.5%) pollens increase at the expense of *Castanopsis*-type (3.3–13.8/5.8%), *Quercus* (E) (5.3–12.3/8.5%), *Ulmus* (0–3.0/1.1%), and *Betula* (0–1.3/0.5%). No notable alterations exist in the pollen percentages of *Tsuga* (0.4–2.1/1.1%), *Picea*/*Abies* (0–2.7/0.8%), and Poaceae (0.4–3.2/2%). The pollen influx values in this zone are the highest of the entire core, reaching 3687–7145/5507 grains cm^{-2} a^{-1}. The first three pollen spectra (subzone 4a) of this zone are characterized by low *Pinus* (42.7–57.1/52.1%) as well as high *Quercus* (E) (7.5–12.3/10.5%), *Castanopsis*-type (4.6–13.8/9.6%), and *Alnus* (6.5–9.8/7.9%) pollen percentages.

Pollen zone FXH-3 (446–194 cm; 11,200–5000 cal. a BP): This zone, consisting of 27 pollen spectra, is characterized by pollen percentage maxima of *Liquidambar* (0–3.6/1.9%), *Ulmus* (0.2–5.2/4.5%), and *Pterocarya* (0–1.8/0.8%), as well as the second minimum of *Pinus* (53.4–82.9/64.5%). It can be further divided into four subzones (446–405, 405–355, 355–245, and 245–194 cm) in terms of pollen percentages of *Ulmus* and *Liquidambar* and pollen influx values. Subzones 4d-a contain less, more, maxima, and less of *Ulmus* and *Liquidambar* pollen, and have high, low, high and low pollen influx values (3637–6564/5039, 3770–5404/4295, 3941–8698/4852, and 1605–4983/3581 grains cm^{-2} a^{-1}).

Pollen zone FXH-2 (194–135 cm; 5000–2500 cal. a BP): In this zone, six pollen spectra are differentiated from those of zone FXH-3 and FXH-1 by the *Pinus* pollen percentage maximum of the entire core (71.2–86.6/81.7%) and significant drops in *Quercus* (E) (2.3–5.4/3.8%), *Quercus* (D) (2–3.9/2.8%), *Castanopsis*-type (1.1–2.5/1.6%), *Alnus* (0.6–2.9/1.5%) and Poaceae pollens (1.2–2.9/2%). *Liquidambar*, *Ulmus*, and *Pterocarya* pollens decline to near nonexistence. The pollen influx values (2636–4589/3720 grains cm^{-2} a^{-1}) are low.

Pollen zone FXH-1 (135–0 cm; 2500 cal. a BP to the present): This zone, consisting of 16 pollen spectra, is marked by a notable non-linear decline of *Pinus* (49.2–79.2/66.6%), a persistent decrease in the pollen influx values, and a distinct rise in herbaceous pollen. *Quercus* (E) (1.5–7.7/4.7%), *Quercus* (D) (1.3–5.6/3.1%), *Castanopsis*-type (1.6–7.3/3.8%), and *Alnus* (1.1–10.3/4.1%) pollens rise at the cost of *Pinus* pollen. *Tsuga*, *Pterocarya*, and *Liquidambar* pollens appear occasionally. The pollen influx values (554–3147/1698 grains cm^{-2} a^{-1}) are at their minimum of the entire core, exhibiting a sharp downward trend. This zone can be further divided into two subzones. Subzone FXH-1a contains more *Alnus* and Poaceae pollens and lower pollen influx values than subzone FXH-1b.

4.3. PA of RVC in the Catchment of Lake Fuxian since the LGM

The REVEALS model was developed to estimate the past PA of the RVC for pollen records from large lakes using fossil pollen counts [35], in which the regional PA is estimated by the weighted pollen counts of each taxon using its pollen production and dispersal terms [57,58]. In the Lake Fuxian catchment of central Yunnan, Poaceae was chosen as the reference taxon; the RPPs of 14 pollen taxa were used to estimate their PAs with the aid of the "disqover" package, as was completed for the Lake Yongzonghai (near Lake Fuxian) catchment [53]. A comparison of the pollen percentage diagram (Figure 4) with the REVEALS-adjusted PA diagram (Figure 6) shows that the arboreal PA (83.4%) is >10% lower than its pollen percentage (97.4%). The PA of *Pinus* is much less (>40%), whereas the PA of *Liquidambar* is much more than its pollen percentages, indicating that the REVEALS adjusts an over- or under-representation of pollen in the plant interpretation, thus reducing the uncertainties in the vegetation interpretation of pollen data. The PAs of the RVC in the pollen zones of core FXH-1 (Figure 6) display the following characteristics:

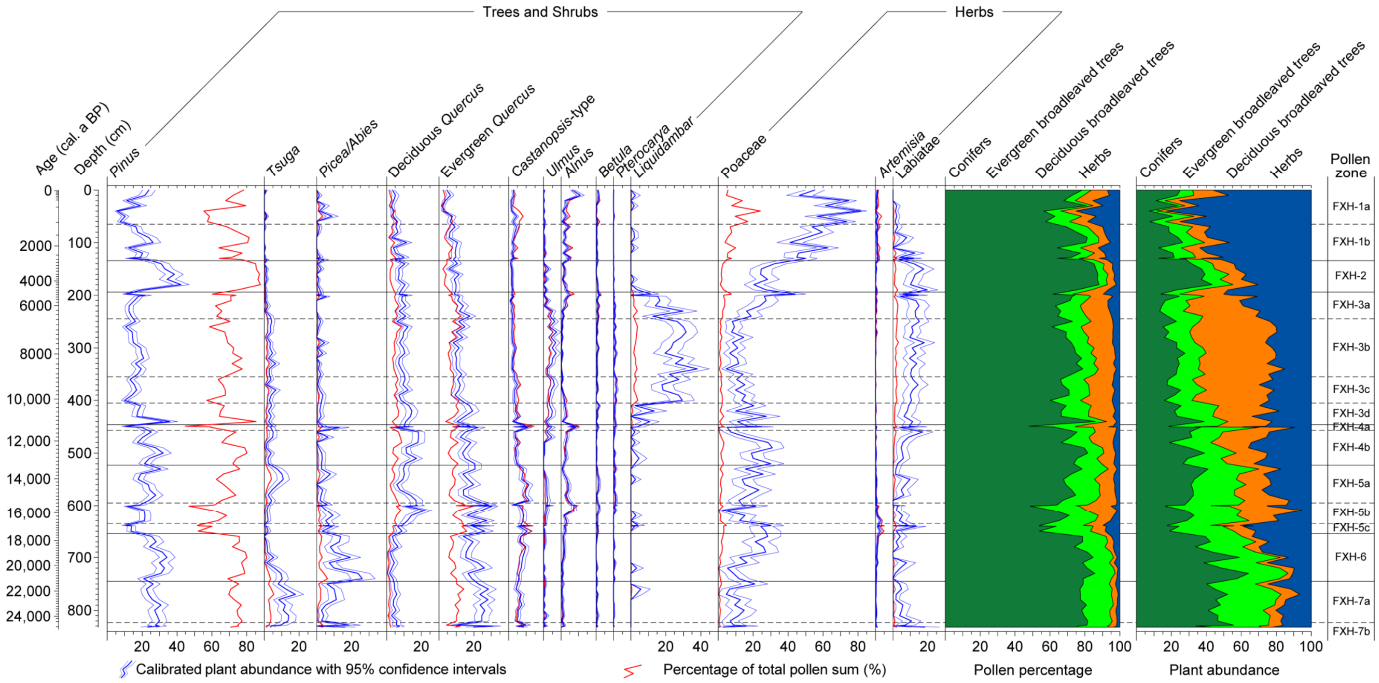

Figure 6. PA diagram of main taxa in the catchment of Lake Fuxian.

Pollen zone FXH-7 (832–745 cm, 25,000–21,200 cal. a BP): Arboreal plants make up 83.4% (the zone average, the same as below) of the regional vegetation composition, in which *Quercus* (E) (23.9%), *Pinus* (26.9%), and *Tsuga* (10.4%), *Picea*/*Abies* (7.9%) are the dominant trees, followed by *Castanopsis*-type (6.3%) and *Quercus* (D) (5.1%). Herbaceous plants (16.6%) are dominated by Poaceae (10.4%) and Labiatae (5.8%).

Pollen zone FXH-6 (745–655 cm; 21,200–17,500 cal. a BP): Arboreal PAs (79.2%) slightly decrease, whereas herbaceous PAs (20.7%) slightly increase. The forests consist of more *Pinus* (28.7%), *Picea*/*Abies* (14.6%), and *Castanopsis*-type (7.4%) and less *Quercus* (E) (18.4%), *Tsuga* (4.2%), and *Quercus* (D) (3.6%). Herbaceous plants are dominated by Poaceae (17.4%).

Pollen zone FXH-5 (655–525 cm; 17,500–13,300 cal. a BP): Arboreal PAs continue to decrease. Among arboreal plants, the vacancy caused by significant decreases of *Pinus* (19.4%) and *Picea*/*Abies* (4.4%) is filled by *Quercus* (E) (20.9%), *Quercus* (D) (11.7%), and *Alnus* (3.7%). Herbaceous plants (24.2%) consist mainly of Poaceae (18.7%) and Labiatae (4.4%).

Pollen zone FXH-4 (525–445 cm, 13,300–11,200 cal. a BP): The PAs of trees (72.1%) slightly decreases, whereas the herbaceous PA (27.9%) slightly increases. The trees are predominated by *Pinus* (21.2%), *Quercus* (E) (16.2%), and *Quercus* (D) (13.3%); *Castanopsis*-type (5.4%), *Alnus* (4%), and *Tsuga* (3.3%) are common. The herbaceous plants still consist mainly of Poaceae (19.8%) and Labiatae (7.8%).

Pollen zone FXH-3 (445–194 cm; 11,200–5000 cal. a BP): Arboreal and herbaceous PAs (72.8% and 27.2%) change little, while their components change significantly. *Liquidambar* and *Ulmus* reach their maxima (20.2% and 3.9%). Other abundant taxa in arboreal plants include *Pinus* (16.6%), *Quercus* (D) (9.8%), *Quercus* (E) (12.1%), *Castanopsis*-type (2.7%), and *Tsuga* (3%). Herbaceous plants are dominated by Poaceae (15.8%) and Labiatae (11.2%). At the depths of 245–235 and 205–199 cm (6800–6400 and 5500–5000 cal. a BP), significant decreases in the abundances of *Liquidambar* (14.6%) and *Tsuga* (1.4%) occur as well as a significant increase in Poaceae (23.9%).

Pollen zone FXH-2 (194–134 cm; 5000–2500 cal. a BP): Arboreal PAs fall to 59.6%, the second lowest level of the entire core. Among trees, the *Pinus* abundance increases from 16.6% of zone FXH-3 to 33.2%, whereas the abundances of *Quercus* (E) (9.4%), *Quercus* (D) (8.4%), and *Castanopsis*-type (1.9%) decrease. *Liquidambar*, *Ulmus*, and *Pterocarya* decline to almost disappearance.

Pollen zone FXH-1 (134–0 cm; 2500 cal. a BP to the present): The PAs of trees decrease further to their lowest level (39.1%) of the whole core. Among trees, *Pinus* (17%), *Quercus* (D) (5.5%), and *Quercus* (E) (7%) decrease; *Liquidambar*, *Ulmus*, and *Pterocarya* tend to disappear; *Alnus* (3.5%) slightly increases. Herbaceous PAs reach their maximum (61%) of the entire core. In herbs, Poaceae (56.5%) dominates, and Labiatae (3.5%) and *Artemisia* (1%) are common.

4.4. Forest Types in the Catchment of Lake Fuxian since the LGM

Lake Fuxian is nestled within the Chengjiang Basin on the central Yunnan Plateau. Fossil pollen of core FXH-1 in Lake Fuxian originated from regional vegetation, especially forests, growing in the catchment of Lake Fuxian. To uncover the forest types in the catchment of Lake Fuxian since the LGM, the PCA of a major pollen dataset, consisting of 96 samples and 14 pollen taxa, was employed. Fourteen major pollen taxa include *Picea*/*Abies*, *Tsuga*, *Pinus*, *Quercus* (D), *Quercus* (E), *Castanopsis*-type (mostly *Castanopsis*/*Lithocarpus*, rarely *Castanea*), *Ulmus*, *Alnus*, *Betula*, *Liquidambar*, *Pterocarya*, Poaceae, *Artemisia*, and Labiatae. The PCA result indicates that the initial two principal components (PCs) account for 26.7% and 22.1% of the variation of this dataset.

The biplot of the initial two PCs (Figure 7) shows the ordination of samples is closely correlated with that of pollen taxa. On one axis, samples with high scores are primarily composed of pollen types with high scores. The first PC axis distinguishes pine forests, fir/spruce forests, and grasslands/wetlands on the negative end from other forest types. Figure 7 also shows that typical pine forests, fir/spruce forests, and grasslands/wetlands are reflected by pollen spectra of zones FXH-7, FXH-6, and FXH-1, respectively. The positive end are DBFs predominated by *Liquidambar*, *Ulmus*, *Pterocarya*, and *Quercus* (D). Those DBFs are reflected by the pollen spectra of zone FXH-3. The second PC axis separates pine forests on the positive end, and EBFs, alder, and birch forests on the negative end. The pollen spectra of zone FXH-2 likely reflect pure pine forests, whereas the pollen spectra of zone FXH-5 reflect EBFs dominated by *Castanopsis*-type and evergreen oak as well as alder and birch forests. The discrete distribution of pollen spectra for most pollen zones, such as zone FXH-4, in the PCA biplot suggests the mixed feature of a variety of pollen sources due to a huge lake catchment.

In the catchment of Lake Fuxian, modern pine forests are dominated by *Pinus yunnanensis* and *P. armandi*. *Pinus yunnanensis* (yunnan pine) forest occurs in areas 1740–2100 m a.s.l., whereas *P. armandi* forest occur in areas of 1900–2300 m [44]. The climatic preference of the Yunnan pine forest is for a dry winter and spring, wet summer and autumn, and small seasonal temperature differences. Therefore, the pine forests inferred from the pollen spectra of different zones may indicate different types of pine forests.

Hemlock forest and fir/spruce forests are cool and cold temperate montane coniferous forests in western Yunnan and northeastern Yunnan. The former grows in mountainous areas 2600–3400 m a.s.l., where the MAT, MAP, and MAH are 6–12 °C, >700 mm, and >75%, respectively; the latter grows in areas 3000–4000 m a.s.l. with an MAT of 4.6–5.3 °C, MAP of around 600 mm, and MAH of around 70% [59]. Hemlock forests and fir/spruce forests indicated by pollen spectra are likely confined to limited areas on mountain summits surrounding Lake Fuxian.

EBFs exhibit a broad distribution range, encompassing northern, central, and southern regions of Yunnan across 3–4 latitudes. Vertically, they thrive at elevations 1000–2800 m a.s.l., covering a vertical gradient of nearly 2000 m. They contain warm EBFs in northern and central Yunnan, where the MAT and MAP are 15–17 °C and 900–1200 mm, and warm–hot EBFs in southern Yunnan, where the MAT and MAP are 17–19 °C and 1100–1700 mm. Warm EBFs are dominated by *Quercus delavayi*, *Castanopsis delavayi*, *C. orthacantha*, *Lithocarpus echinotholus*, *L. craibianus*, and *L. variolosus* along with *Quercus aliena*, *Q. dentata*, *Q. griffithii*, *Q. acutissima*, and *Q. variabilis*. Warm–hot EBFs are dominated by *Castanopsis hystrix*, *C. indica*, *C. fluryi*, *Lithocarpus truncatus*, *Schima wallichii*, and *S. villosa*. EBFs reflected by

the pollen spectra involve presumably warm and warm–hot EBFs before and after the Holocene, respectively.

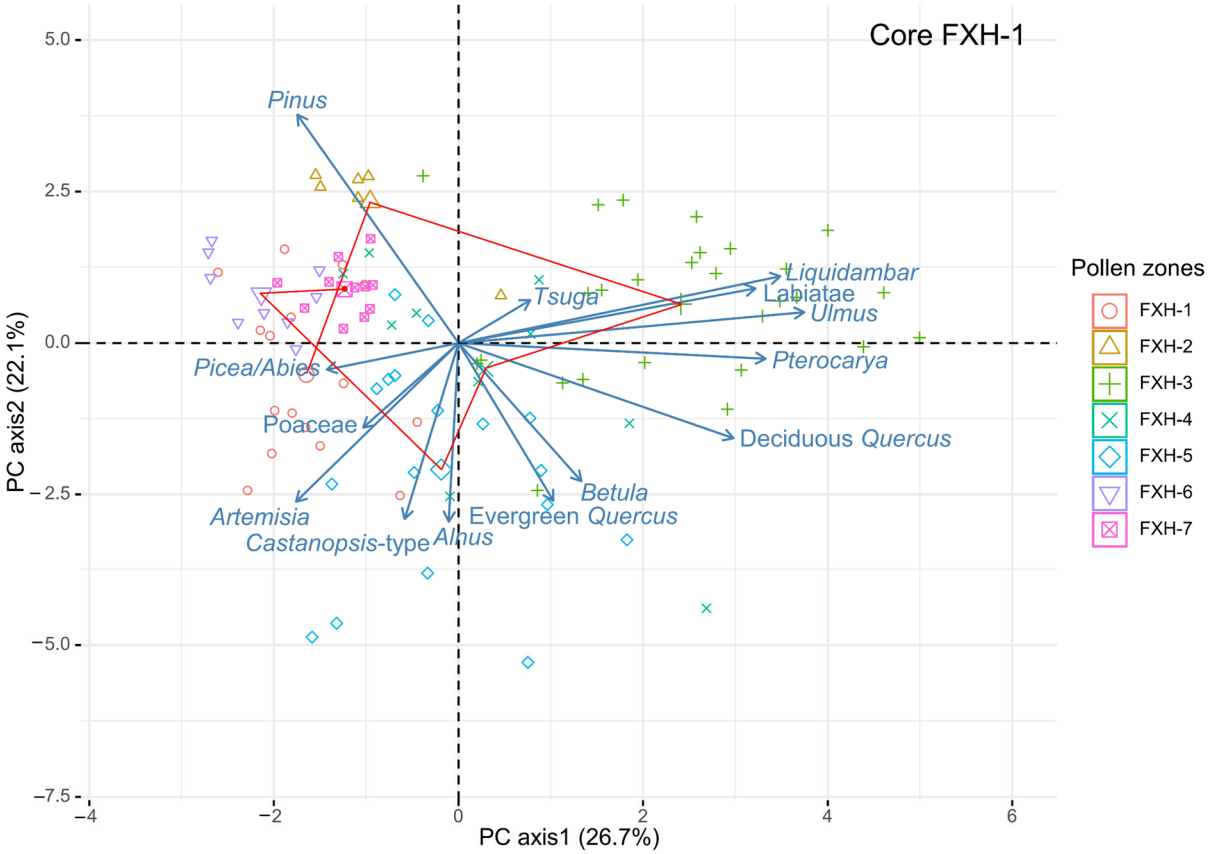

Figure 7. Biplot of PCA on pollen percentages of 14 main pollen taxa from core FXH-1 in Lake Fuxian. The red lines represent the trajectory of vegetation change, indicated by pollen zone centers.

DBFs are also extensively distributed throughout Yunnan. They include cold–temperate, cool–temperate, warm, and warm–hot DBFs. *Betula albo-sinensis*, *B. platyphylla*, *Quercus pannosa*, and *Q. aquifolioides* are common cold–temperate forests at 2800–3500 m a.s.l. in northwest Yunnan, with a MAT of <10 °C and MAP of 700–900 mm. *Quercus dentata* and *Acer* spp. forests are common cool–temperate ones at 2300–3500 a.s.l. in west and northwest Yunnan, where the MAT and MAP are 7–12 °C and 900–1000 mm. Warm DBFs, such as *Quercus acutissima*, *Q. aliena*, *Q. variabilis*, *Juglans sigillata*, and *Alnus nepalensis* forests, are usually secondary forests after the disturbance of EBFs. *Liquidambar formosana* and *Betula alnoides* forests are two primary warm–hot DBFs growing on hilly or mountainous terrains at 1500–2000 m a.s.l., with a MAT of 16–20 °C and MAP of 1100–1700 mm. DBFs reflected by fossil pollen spectra should include oak, alder, birch, elm, wingnut, and sweetgum forests.

4.5. Regional Vegetation Dynamics in the Catchment of Lake Fuxian since the LGM

As shown in Figure 8, the regional vegetation dynamics since the LGM in the catchment of Lake Fuxian experienced seven stages:

Stage 7 (25,000–21,200 cal. a BP; pollen zone FXH-7): In the catchment of Lake Fuxian, its hilly terrains were covered by EBFs, DBFs, and pine forests, and the summits of mountains surrounding the lake by cool–temperate montane hemlock forests and cold-temperate montane fir/spruce forests; its southern and northern lowlands are occupied by grass wetlands or grasslands. EBFs of ca. 30.2% of the RVC (the zone average, the same as below) were dominated by evergreen oak, *Castanopsis*, and *Lithocarpus*, along with some DB trees and shrubs. DBFs of ca. 8% were composed of deciduous oaks,

alder, birch, and elm. Pine forests of ca. 26.9% was probably predominated by *Pinus armandi*, together with some likely *P. yunnanensis*. Montane hemlock forests (ca. 10.4%) and fir/spruce forests (ca. 7.9%) were the first and second maxima of the entire sequence. Grass wetlands and grasslands of ca. 16.6% were dominated by Poaceae, Labiatae, and *Artemisia*. The vegetation density, as indicated by the pollen influx values, was low in this stage. However, a high vegetation density with more fir/spruce forests (ca. 11.6%) occurred at 25,000–24,400 cal. a BP, suggesting the occurrence of an abrupt centennial vegetation shift event (ACVSE).

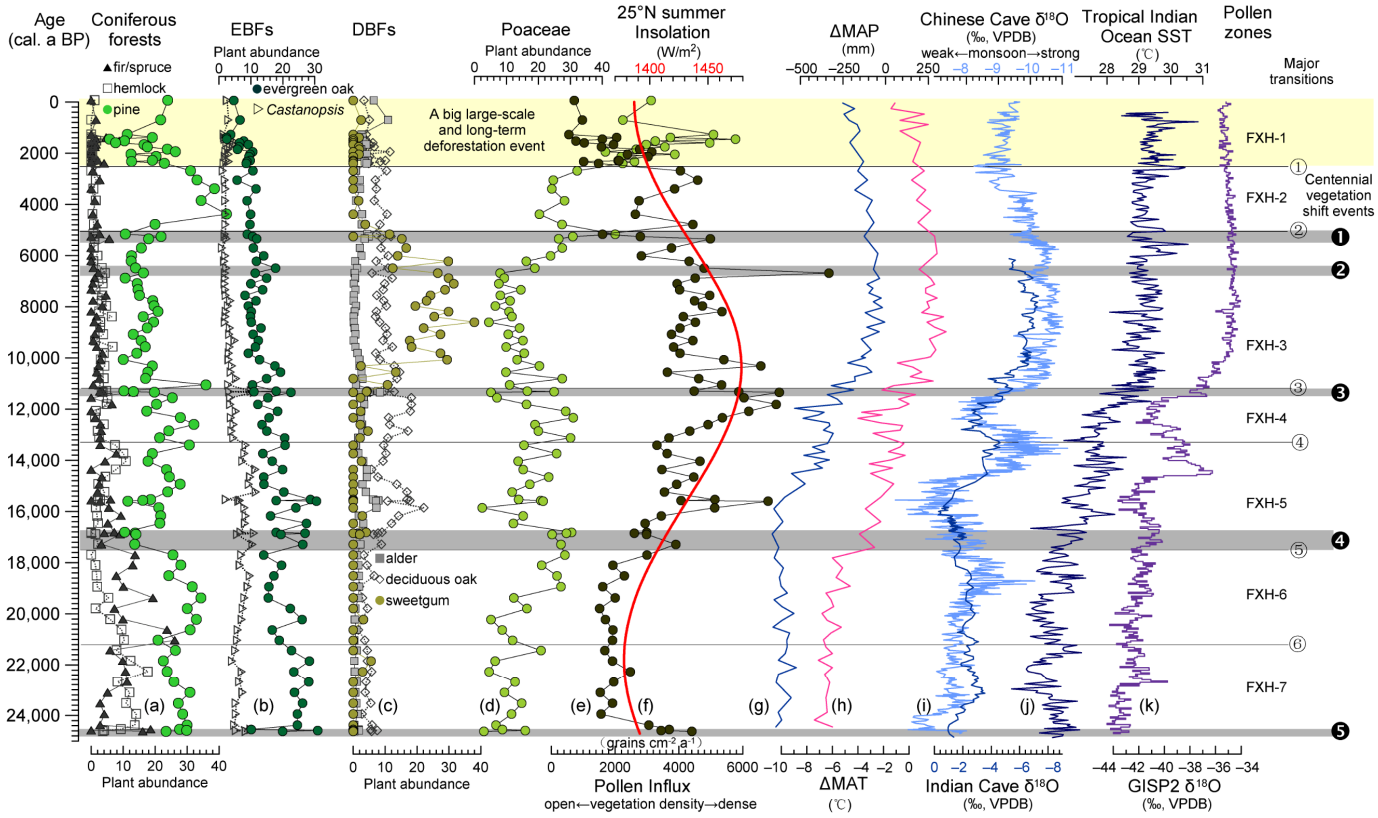

Figure 8. A comparison of the plant abundances and vegetation density of different vegetation types with regional climatic conditions, summer insolation, monsoon intensity, ocean SST (sea surface temperature), and temperature of Greenland since the LGM: (**a**) coniferous forests, (**b**) EBFs, (**c**) DBFs, (**d**) grassland and wetland, (**e**) total pollen influx (a proxy of vegetation density) of this study; (**f**) 25° N summer insolation (W/m^2) [60], ΔMAP (**g**), and ΔMAT (**h**) in the Lake Qinghai catchment of west Yunnan [61], (**i**) a composite Chinese cave $\delta^{18}O$ record (a proxy of Asian monsoon intensity) [62] and an Indian cave $\delta^{18}O$ record (a proxy of South Asian monsoon intensity) [63], (**j**) tropical Indian Ocean SST [64], and (**k**) a GISP2 $\delta^{18}O$ record in Greenland [65] (a proxy of temperature of high latitude in the Northern Hemisphere).

Stage 6 (21,200–17,500 cal. a BP; pollen zone FXH-6): EBFs (ca. 25.8%), DBFs (ca. 6.0%), and montane hemlock forests (ca. 4.2%) shrank, whereas pine forests (ca. 28.7%) and montane fir/spruce forests (ca. 14.6%), as well as grasslands and grass wetlands (ca. 20.7%), expanded in the lake catchment. In pine forests, *Pinus armandi* likely still had greater presence than *P. yunnanensis*. The vegetation density was still as low as that of the previous stage.

Stage 5 (17,500–13,300 cal. a BP; pollen zone FXH-5): EBFs (ca. 29.1%) and DBFs (ca. 19.2%) expanded at the expense of pine forests (ca. 19.4%) and montane hemlock and fir/spruce forests (ca. 3.7% and 4.4%). Among DBFs, deciduous oak forests (ca. 11.7%) and alder forests (ca. 3.7%) significantly increased. In pine forests, *Pinus armandi* was

presumably replaced by *P. yunnanensis* gradually. The forest density increased to become dense. Grasslands and grass wetlands (ca. 24.2%) slightly expanded. A quick expansion of EBFs (ca. 31.2%) and DBFs (ca. 12.9%), as well as grasslands and grass wetlands (ca. 36.2%), and an abrupt decline in pine forests (ca. 12.9%), montane hemlock forests, and fir/spruce forest (ca. 0.9% and 5.9%) occurred at the onset of this stage from 17,500 to 16,700 cal. a BP, implying an ACVSE.

Stage 4 (13,300–11,200 cal. a BP; pollen zone FXH-4): Grasslands and grass wetlands (ca. 27.9%) and DBFs (ca. 22.5%) expanded slightly at the cost of EBFs (ca. 21.6%). Pine forests (21.2%), montane hemlock forests, and fir/spruce forests (ca. 3.3% and 3.6%) changed a little. However, sweetgum forests began to invade the lake catchment. The vegetation density became denser and denser, reaching its maximum. At the end of this stage from 11,500 to 11,200 cal. a BP, the lake catchment witnessed a quick expansion of EBFs and alder forests and a fast reduction in pine forests and grasslands, indicating another ACVSE.

Stage 3 (11,200–5000 cal. a BP; pollen zone FXH-3): Sweetgum forests expanded non-linearly to their maximum (ca. 20.2%) of the whole series at 10,000–6500 cal. a BP and then declined non-linearly to almost disappearance. Pine forests (ca. 16.6%) and EBFs (ca. 14.8%) shrank, whereas montane hemlock forests and fir/spruce forests (ca. 3.0% and 1.6%) as well as grasslands and grass wetlands (ca. 27.2%) maintained their presence from the previous stage. The vegetation density was unchanged from that of the previous stage until 6500 cal. a BP, when it became progressively less dense. In this stage, the periods of 6800–6400 and 5500–5000 cal. a BP saw abrupt declines in sweetgum forests and the vegetation density as well as great expansions of grasslands and wetlands, implying another two ACVSEs.

Stage 2 (5000–2500 cal. a BP; pollen zone FXH-2): Pine forests (ca. 33.2%) expanded quickly to reach a maximum of the complete sequence, whereas DBFs (ca. 13.1%) and EBFs (ca. 11.3%) thinned. Among DBFs, sweetgum forests rapidly declined to almost vanish. Montane hemlock forests and fir/spruce forests appear occasionally. Grasslands and wetlands (ca. 40.4%) expanded significantly. The vegetation density exhibited a high–low–high pattern but much lower than those of the previous three stages.

Stage 1 (2500 cal. a BP to the present; pollen zone FXH-1): After 2500 cal. a BP, pine forests contracted swiftly to their lowest of the whole series around 1500 cal. a BP and then rose again. Overall, the forests displayed non-linear decline patterns up to the present, whereas grasslands and wetlands (ca. 60.9%) expanded to their maxima. The minimum vegetation density of the entire sequence occurred in this period. The unusually high presence of Poaceae (ca. 56.5%) in this stage should be related to the great increase of cultivated vegetation.

Overall, the regional vegetation dynamics since the LGM in the catchment of Lake Fuxian experienced seven stages of vegetation changes in forest types as well as grasslands and wetlands. Stage 7 saw a regional vegetation predominated by EBFs, DBFs, and coniferous forests, including pine forests, montane hemlock forests, and fir/spruce forests. Stage 6 saw an expansion of grasslands and a shrinkage of EBFs and DBFs. Stage 5 witnessed the expansion of deciduous oak and alder forests as well as EBFs. The regional vegetation in stage 4 was dominated by pine forests, DBFs, grasslands and wetlands. Sweetgum forests and pine forests reached their maximums in stages 3 and 2, respectively. A big deforestation happened in stage 1, when grasslands, wetlands, and cultivated vegetation dominated the regional vegetation in the catchment of Lake Fuxian.

5. Discussion

The Lake Fuxian pollen record uncovers seven stages of relatively stable regional vegetation (corresponding to seven pollen zones), six significant vegetation transitions (equivalent to six pollen zone boundaries), five ACVSEs, and a big deforestation event (Figure 8).

5.1. Regional Vegetation Dynamics in the Lake Fuxian Catchment since the LGM in Response to Climate Change

Stage 7 of 25,000–21,200 cal. a BP corresponds roughly to the early LGM, when Yunnan experienced the coldest MAT and lowest MAP (Figure 8g,h). The reconstructed MATs and MAPs from fossil pollen spectra of Lake Qinghai (Tengchong) in west Yunnan were >6 °C and >600 mm lower than their contemporary values in this stage [61] during the following occurrences: the minimum of summer insolation of 25° N [60], coldest tropical Indian Ocean SST [64] and Greenland air temperature, and the weakest Asian and South Asian summer monsoons [62,63,66]. In this study, the redness of lake sediments at this stage (Figure 3), a proxy of erosion intensity [55], shows subdued surface erosions in the lake catchment, implying harsh climatic conditions. The lake catchment under such climatic conditions was occupied by the maximum evergreen oak forest (likely evergreen sclerophyllous oak forest, in a similar situation to the Lake Qinghai catchment in west Yunnan [31]) and the first and second maxima of the montane hemlock forest and fir/spruce forest of the entire sequence, indicating the response of the forests to climate changes. The same fact was also found in other lake catchments at this stage. In northwest Yunnan, vegetation at this stage was dominated by sparse grasslands in the catchments of Lakes Shudu [29] and Lugu [28], where montane fir/spruce forests and evergreen sclerophyllous oak forests grow at present under climatic conditions of MATs of 15 and 12.9 °C and MAPs of 600 and 1000 mm. In west Yunnan, evergreen sclerophyllous oak forests dominated the Lake Qinghai catchment, where modern vegetation in the lake catchment is warm EBFs under climatic conditions of an MAT and MAP of 15.4 °C and 1500 mm [31]. In central and southern Yunnan, the regional vegetation at this stage was dominated by fir/spruce forests, EBFs, and DBFs in the catchments of Lakes Xingyun and Yilong, where semi-humid, warm EBFs and Yunnan pine grow today under climatic conditions of MATs of 16.1 and 18 °C and MAPs of 870 and 928 mm. Interestingly, an ACVSE at 25,000–24,400 cal. a BP seems to occur with a transient amelioration of climatic conditions, as shown in Figure 8.

Stage 6 of 21,200–17,500 cal. a BP is equal to the late LGM, when the MAT and MAP still were low in Yunnan. However, regional vegetation in the Lake Fuxian catchment experienced a major transition from hemlock-dominated to fir/spruce-dominated forests and a gradual uptrend in the vegetation density, which seemingly followed the increasing trend of summer insolation. A similar pattern was also found in the regional vegetation of the Lake Xingyun catchment [33].

Stage 5 of 17,500–13,300 cal. a BP is the last deglaciation following the LGM. In the last deglaciation, the MAT and MAP became higher and higher in Yunnan [61,67], while Asian and South Asian monsoons weakened and then strengthened. Regional vegetation in the catchments of Lakes Fuxian, Xingyun [33], and Dianchi [32] experienced a major transition from montane forests dominated by hemlock, fir/spruce, and pine to broadleaved forests dominated by *Castanopsis*, evergreen, and deciduous oaks. The vegetation density in the Lake Fuxian catchment of this stage was about twice as much as the previous stage, markedly following the increase of summer insolation, the amelioration of regional and global climatic conditions, and the strengthening of Asian and South Asian summer monsoons. The regional vegetation witnessed a significant increase of birch/hornbeam forests in the catchments of Lakes Shudu, Lugu, and Qinghai of west and northwest Yunnan, reflecting the response of the vegetation to climate changes. Interestingly, a quick expansion of EBFs and DBFs and an abrupt decline in pine forests, montane hemlock forests, and fir/spruce forests as well as a major drop in the vegetation density occurred in a period of less than 800 years from 17,500 to 16,700 cal. a BP, probably implying the response of regional vegetation to Heinrich event 1 [65].

Stage 4 of 13,300–11,200 cal. a BP is roughly equal to the Younger Dryas Chron geochronologically. Climatic conditions during this stage were characterized by a drop in the regional and hemispheric temperatures (including the air temperature and SST) and regional precipitation, as well as the weakening of summer monsoons. This change is also widely recorded in Yunnan [14,68,69]. The regional vegetation in the catchment of

Lake Fuxian underwent another significant vegetation transition, from broadleaved forest-dominated to pine forest and grassland-dominated vegetation and an ever-increasing trend of vegetation density through the entire stage. In the catchments of Lakes Xingyun [33] and Dianchi [32], more hemlock, fir/spruce, and birch forests occurred in the regional vegetation, and the vegetation density of this stage was about twice as much as the previous stage. It seems expected that the regional vegetation changed in response to climate change. Interestingly, this stage saw a high vegetation density. An explanation of this fact is that this stage is in the 25° N summer insolation maximum period of ca. 12,000–9000 cal. a BP and growing-season warming, thus favoring vegetation to flourish. This explanation seems reasonable, since the total pollen influx values and 25° N summer insolation changed synchronously over the last 25,000 years, as shown in Figure 8e,f. An alternative explanation is that climatic conditions during the Younger Dryas favored the growth of forests and grasslands in central Yunnan. The end of this stage from 11,500 to 11,200 cal. a BP saw a quick expansion of EBFs and alder forests, a fast shrinking of pine forests and grasslands, and a great drop in the vegetation density, probably implying a centennial cold event as indicated by the MAT in the Lake Qinghai catchment and Indian Ocean SST.

Stage 3 of 11,200–5000 cal. a BP corresponds to the early–mid-Holocene, characterized by global warming and the intensification of the Asian summer monsoon [70]. The regional vegetation in the catchment of Lake Fuxian experienced another major vegetation transition from pine forests and grassland-dominated vegetation to sweetgum forest and DBF-dominated vegetation at 11,200 cal. a BP. Similar vegetation change patterns involving sweetgum forests and other warm DBFs were also found in the response of regional vegetation dynamics to climate changes in the catchments of Lakes Xingyun [33], Dianchi [32], Yangzonghai [71], Yilong [72], and Qinghai [31]. The sweetgum forest is a warm–hot DBF, favoring hot and wet climatic conditions in hilly terrains, where the MAP is 900–1200 mm and the MAT is 16–20 °C, with an extremely warm temperature of ca. 36 °C [59]. Obviously, its appearance and expansion to its maximum of the entire sequence in central Yunnan resulted from the regional vegetation response to the amelioration of climatic conditions during the early–mid–Holocene. During this stage, two ACVSEs characterized by abrupt declines in the sweetgum forests and vegetation density as well as great expansions of grasslands and wetlands occurred at 6800–6400 and 5500–5000 cal. a BP. The first event might be associated with a regional cold event around 6.5 cal. ka BP [73]; the second event was probably related to a weak South Asian summer monsoon event [74,75].

Stage 2 of 5000–2500 cal. a BP is the early period of the late Holocene. In this stage, the MAT and MAP became lower and lower in Yunnan, and Asian and South Asian monsoons weakened [74,76,77]. The regional vegetation changed from sweetgum forest-dominated to pine forest-dominated in the catchments of Lake Fuxian and other lakes in central Yunnan [32,33,71,72]. It is certain that the regional vegetation change in this stage was the response of the vegetation to a deteriorative climate. Furthermore, the vegetation density after 5000 cal. a BP also exhibited a non-linear downward trend following summer insolation and the deterioration of climatic conditions.

During the Holocene, North Atlantic and monsoon Asia experienced a series of centennial cold/monsoon weakening events [22,78–82]. Among them, the events around 11,000, 6500, and 5300 cal. a BP left their footprints on the regional vegetation of the Lake Fuxian catchment. However, most of them did not leave significant proofs in the regional vegetation, especially the events lasting several centuries, such as 8.2, 4.2, and 2.8 ka events, although some events may leave their hints in the regional vegetation, such as a drop in the sweetgum abundance around 8.2 cal. ka BP, presumedly implying the 8.2 ka event. This phenomenon is thus probably caused by (1) a limited sampling resolution, (2) a limited amplitude of climate events, (3) a limited sensitivity of vegetation to climate change, and (4) the lack of definite criteria to define an event using vegetation proxies.

5.2. Regional Vegetation Dynamics in the Lake Fuxian Catchment since 2500 cal. a BP in Response to Human Activities

Stage 1 of 2500–0 cal. a BP is the late period of the late Holocene with the lowest MAP and MAT of the Holocene. The regional vegetation experienced a major transition from forest-dominated to grassland and wetland-dominated at 2500 cal. a BP. The forests thinned after 2500 cal. a BP to reach their minima around 1500 cal. a BP, implying that a big large-scale and long-term deforestation event happened in central Yunnan at this stage. The redness of lake sediments showed a pronounced peak after 2500 cal. a BP, aligning with elevated magnetic susceptibility, suggesting the degradation of basin vegetation and the exacerbation of soil erosion due to human activities during this stage [55]. This deforestation event, initiated as early as 2500 cal. a BP, reached its maximum at ca. 1500 cal. a BP and probably has not yet ended. This interpretation is supported by proxies of human activities from adjacent lakes, archaeological evidence, and historical documents. In the catchment of Lake Xingyun, the comprehensive suite of biogeochemical and isotopic proxies indicates that human activities have profoundly affected the lake for >1500 years [83]. Human activities around Lake Qilu, located approximately 17 km away from the Lake Fuxian, were also be dated back to around 1500 cal. a BP, when this lake bore distinctive anthropogenic influences, manifesting in the transportation of red and iron-rich catchment soil into the lake and exhibiting elevated oxygen isotope values. These changes are likely the result of land clearance for the expansion of agricultural activities [84]. Several archaeological sites such as the Anjiang site (2520–2470 cal. a BP) [85], Dayingzhuang site (2580–2400 cal. a BP) [86], and Yangputou site (2570–2030 cal. a BP) [87] were found in the Lake Fuxian catchment. Bronze culture reached its highest level and began the transition to the Iron Era in the Dianchi area around 2200 BP (before present), when much of the coal required for bronze and/or iron smelting was sourced from cutting down a considerable number of trees [88]. In 279 BC (2229 BP), Qiao Zhuang, a general of the Chu kingdom in the middle Yangtze River, led his army into the Dianchi and Lake Fuxian catchments of central Yunnan, and he eventually became King of the Dian kingdom and brought the advanced culture and production technology of the Chu kingdom to central Yunnan, accelerating the local social and economic development [89]. Dian became a vassal kingdom of Han China at 2090 BP. Wen Chi, the Han administrator of the central Yunnan, firstly introduced terraced and watered fields at approximately 1780 BP. Around 1290 BP, the people of Nan Zhao in the catchment of Lake Erhai increasingly migrated into central Yunnan, and a city named Tue Dong near the northern shore of Lake Dianchi was established at 1230 BP. A total of 10,000 families of North China came to central Yunnan thirty years later, when wheat was cultivated on the terraced hillsides and rice in the valleys; as well, brooks and streams were utilized for irrigation [90]. In the Ming and Qing dynasties, mass migrations into Yunnan occurred, resulting in the growth of the population and the development of agriculture, and the demand for land increased significantly, making deforestation and the enlargement of cultivable land unavoidable. Since then, the PAs and vegetation densities of forests have never returned to the level at 2500 cal. a BP, even recently.

Overall, there is a marked response of regional vegetation in the Lake Fuxian catchment to both regionally cooling/warming and weakening/strengthening Asian summer monsoons. However, the vegetation density in the lake catchment and summer insolation of 25° N change synchronously without obvious lag. During the last 2500 years, human activities became the dominant force controlling the vegetational dynamics and density.

6. Conclusions

In this study, a pollen analysis of core FXH-1 was carried out to uncover regional vegetation dynamics since the LGM in the Lake Fuxian catchment. The following conclusions were obtained:

1. The results of the cluster analysis and PCA on pollen percentage taxa show that fossil pollen spectra of core FXH-1 can be divided into seven pollen zones distinctly.

2. The PAs estimated from the REVEALS model exhibit this model's applicability in assisting the vegetational interpretation of fossil pollen data.
3. This study reveals that the vegetation dynamics since the LGM in the Lake Fuxian catchment experienced seven relatively stable stages, six major transitions, five centennial shift events, and one big large-scale and long-term deforestation event.
4. In the Lake Fuxian catchment, 25,000–21,200 cal. a BP saw some EBFs, DBFs, pine forests, hemlock forests, and fir/spruce forests, as well as few grasslands and wetlands; 21,200–17,500 cal. a BP witnessed remarkable expansions of pine forests and fir/spruce forests; a great expansion of DBFs and EBFs occurred at 17,500–13,300 cal. a BP; the expansion of pine forests and alder forests as well as the shrinkage of EBFs and hemlock forests occurred at 13,300–11,200 cal. a BP; during 11,200–5000 cal. a BP, sweetgum forests reached their maximum of the last 25,000 years; during 5000–2500 cal. a BP, pine forests reached their maximum of the entire sequence, and sweetgum forests diminished to near absence. The last 2500 years saw a big deforestation event.
5. Vegetation density in the lake catchment has changed synchronously with summer insolation of 25° N since the LGM.
6. Regional vegetation dynamics since the LGM in the Lake Fuxian catchment were associated with hydrothermal conditions during 25,000 to 2500 cal. a BP and human activities during the last 2500 years.

Author Contributions: Conceptualization, C.S.; methodology, M.W., Q.S., H.M., H.Z. and H.S.; software, M.W. and Q.S.; validation, M.W., Q.S. and H.M.; formal analysis, M.W. and Q.S.; investigation, Q.S., H.M., L.H. and H.Z.; resources, M.W., H.M., L.H. and H.S.; data curation, M.W. and Q.S.; writing—original draft preparation, M.W.; writing—review and editing, C.S. and Q.S.; visualization, M.W. and L.H.; supervision, C.S. and H.Z.; project administration, C.S.; funding acquisition, C.S., H.M., M.W. and H.S. All authors have read and agreed to the published version of the manuscript.

Funding: This research was funded by the National Natural Science Foundation of China: 42177437, 42167065, 41971115, 41372191, and 41761044; the Special Project for Basic Research of Yunnan Province—Key Project: 202101AS070006; the Youth Talent Support Program of Xingdian Talent Plan Yunnan Provence: XDYC-QNRC-2022-0029; the Yunnan Project for the Introduction of Advanced Talents: 2013HA024; the Yunnan Normal University Postdoctoral Research Project; the Yunnan Normal University Faculty of Geography Postdoctoral Fund: YNNU-FG-201; and the Yunnan Normal University Faculty of Geography Open Fund: YNNU-FG-202.

Data Availability Statement: The datasets used and generated in this study are available from the corresponding author upon reasonable request.

Acknowledgments: We thank the three anonymous reviewers for their constructive comments and suggestions. We thank Kenneth Z. Shen for his helpful review and English improvements in the manuscript. We also thank all members of the Lake Fuxian coring group for their help with field work.

Conflicts of Interest: The authors declare no conflicts of interest.

References

1. Kunming Institute of Ecology, Chinese Academy of Sciences, Agricultural Regionalization Commission Office of Yunnan Province. *Vegetation Ecological Landscapes of Yunnan*; China Forestry Publishing House: Beijing, China, 1994. (In Chinese)
2. Wu, Z.; Zhu, Y.; Jiang, H. (Eds.) *Yunnan Vegetation*; Science Press: Beijing, China, 1987. (In Chinese)
3. Wang, Y. *Mountain Climate of Yunnan*; Yunnan Science and Technology Press: Kunming, China, 2006. (In Chinese)
4. Tang, C.Q. *The Subtropical Vegetation of Southwestern China: Plant Distribution, Diversity and Ecology*; Springer: Dordrecht, The Netherlands, 2015.
5. Mittermeier, R.A.; Turner, W.R.; Larsen, F.W.; Brooks, T.M.; Gascon, C. Global Biodiversity Conservation: The Critical Role of Hotspots. In *Biodiversity Hotspots: Distribution and Protection of Conservation*; Zachos, F.E., Habel, J.C., Eds.; Springer: Heidelberg, Germany, 2011.
6. Tang, L.; Shen, C.; Lu, H.; Li, C.; Ma, Q. Fifty years of Quaternary palynology in the Tibetan Plateau. *Sci. China Earth Sci.* **2021**, *64*, 1825–1843. [CrossRef]
7. Walker, D. Late Pleistocene-early Holocene vegetational and climatic changes in Yunnan Province, southwest China. *J. Biogeogr.* **1986**, *13*, 477–486. [CrossRef]

8. Lin, S.; Qiao, Y.; Walker, D. Late Pleistocene and Holocene vegetation history at Xi Hu, Er Yuan, Yunnan Province, southwest China. *J. Biogeogr.* **1986**, *13*, 419–440.
9. Sun, X.; Wu, Y.; Qiao, Y.; Walker, D. Late Pleistocene and Holocene vegetation history at Kunming, Yunnan province, southwest China. *J. Biogeogr.* **1986**, *13*, 441–476.
10. Liu, J.; Tang, L.; Qiao, Y.; Head, M.J.; Walker, D. Late Quaternary vegetation history at Menghai, Yunnan province, southwest China. *J. Biogeogr.* **1986**, *13*, 399–418.
11. Birks, H.J.B.; Birks, H.H. *Quaternary Palaeoecology*; Edward Arnold: London, UK, 1980.
12. Shen, J.; Jones, R.T.; Yang, X.; Dearing, J.A.; Wang, S. The Holocene vegetation history of Lake Erhai, Yunnan province southwestern China: The role of climate and human forcings. *Holocene* **2006**, *16*, 265–276. [CrossRef]
13. Song, X.; Yao, Y.; Wortley, A.H.; Paudayal, K.N.; Yang, S.; Li, C.; Blackmore, S. Holocene vegetation and climate history at Haligu on the Jade Dragon snow mountain, Yunnan, SW China. *Clim. Change* **2012**, *113*, 841–866. [CrossRef]
14. Xiao, X.; Haberle, S.G.; Shen, J.; Yang, X.; Han, Y.; Zhang, E.; Wang, S. Latest Pleistocene and Holocene vegetation and climate history inferred from an alpine lacustrine record, northwestern Yunnan Province, southwestern China. *Quat. Sci. Rev.* **2014**, *86*, 35–48. [CrossRef]
15. Chen, F.; Chen, X.; Chen, J.; Zhou, A.; Wu, D.; Tang, L.; Zhang, X.; Huang, X.; Yu, J. Holocene vegetation history, precipitation changes and Indian Summer Monsoon evolution documented from sediments of Xingyun Lake, south-west China. *J. Quat. Sci.* **2014**, *29*, 661–674. [CrossRef]
16. Yang, Y.; Zhang, H.; Chang, F.; Meng, H.; Pan, A.; Zheng, Z.; Xiao, R. Vegetation and climate history inferred from a Qinghai Crater Lake pollen record from Tengchong, southwestern China. *Palaeogeog. Palaeoclim. Palaeoecol.* **2016**, *461*, 1–11. [CrossRef]
17. Xiao, X.; Haberle, S.G.; Li, Y.; Liu, E.; Shen, J.; Zhang, E.; Yin, J.; Wang, S. Evidence of Holocene climatic change and human impact in northwestern Yunnan Province: High-resolution pollen and charcoal records from Chenghai Lake, southwestern China. *Holocene* **2018**, *28*, 129–137. [CrossRef]
18. Shi, Q.; Shen, C.; Meng, H.; Huang, L.; Sun, Q. A 1640-Year vegetation and fire history of the Lake Haixihai catchment in northwestern Yunnan, Southwest China. *Forests* **2023**, *14*, 990. [CrossRef]
19. Liao, M.; Li, K.; Ni, J.; Zhang, Y.; Li, Y. An abrupt vegetation change on south-central Yunnan Plateau (Southwest China) during the last deglaciation. *Palaeogeog. Palaeoclim. Palaeoecol.* **2024**, *641*, 112130. [CrossRef]
20. Clark, P.U.; Dyke, A.S.; Shakun, J.D.; Carlson, A.E.; Clark, J.; Wohlfarth, B.; Mitrovica, J.X.; Hostetler, S.W.; McCabe, A.M. The Last Glacial Maximum. *Science* **2009**, *325*, 710–714. [CrossRef] [PubMed]
21. Clark, P.U.; Shakun, J.D.; Baker, P.A.; Bartlein, P.J.; Brewer, S.; Brook, E.; Carlson, A.E.; Cheng, H.; Kaufman, D.S.; Liu, Z.; et al. Global climate evolution during the last deglaciation. *Proc. Natl. Acad. Sci. USA* **2012**, *109*, E1134–E1142. [CrossRef]
22. Mayewski, P.A.; Rohling, E.E.; Stager, J.C.; Karlén, W.; Maasch, K.A.; Meeker, L.D.; Meyerson, E.A.; Gasse, F.; van Kreveld, S.; Holmgren, K.; et al. Holocene climate variability. *Quat. Res.* **2004**, *62*, 243–255. [CrossRef]
23. Rasmussen, S.O.; Bigler, M.; Blockley, S.P.; Blunier, T.; Buchardt, S.L.; Clausen, H.B.; Cvijanovic, I.; Dahl-Jensen, D.; Johnsen, S.J.; Fischer, H.; et al. A stratigraphic framework for abrupt climatic changes during the Last Glacial period based on three synchronized Greenland ice-core records: Refining and extending the INTIMATE event stratigraphy. *Quat. Sci. Rev.* **2014**, *106*, 14–28. [CrossRef]
24. Bond, G.; Kromer, B.; Beer, J.; Muscheler, R.; Evans, M.N.; Showers, W.; Sharon Hoffmann, S.; Lotti-Bond, R.; Hajdas, I.; Bonani, G. Persistent solar influence on North Atlantic climate during the Holocene. *Science* **2001**, *294*, 2130–2136. [CrossRef] [PubMed]
25. Bosson, J.B.; Huss, M.; Cauvy-Fraunié, S.; Clément, J.C.; Costes, G.; Fischer, M.; Poulenard, J.; Arthaud, F. Future emergence of new ecosystems caused by glacial retreat. *Nature* **2023**, *620*, 562–569. [CrossRef]
26. Dallmeyer, A.; Kleinen, T.; Claussen, M.; Weitzel, N.; Cao, X.; Herzschuh, U. The deglacial forest conundrum. *Nat. Commun.* **2022**, *13*, 6035. [CrossRef]
27. Bova, S.; Rosenthal, Y.; Liu, Z.; Godad, S.P.; Yan, M. Seasonal origin of the thermal maxima at the Holocene and the last interglacial. *Nature* **2021**, *589*, 548–553. [CrossRef]
28. Shen, J.; Xiao, X. Evolution of the South Asian monsoon during the last 20 ka recorded in lacustrine sediments from Southwestern China. *Quat. Sci.* **2018**, *38*, 799–820. (In Chinese)
29. Cook, C.G.; Jones, R.T.; Langdon, P.G.; Leng, M.J.; Zhang, E. New insights on Late Quaternary Asian palaeomonsoon variability and the timing of the Last Glacial Maximum in southwestern China. *Quat. Sci. Rev.* **2011**, *30*, 808–820. [CrossRef]
30. Yao, Y.; Song, X.; Wortley, A.H.; Blackmore, S.; Li, C. A 22 570-year record of vegetational and climatic change from Wenhai Lake in the Hengduan Mountains biodiversity hotspot, Yunnan, Southwest China. *Biogeosciences* **2015**, *12*, 1525–1535. [CrossRef]
31. Zhang, X.; Zheng, Z.; Huang, K.; Yang, X.; Tian, L. Sensitivity of altitudinal vegetation in southwest China to changes in the Indian summer monsoon during the past 68000 years. *Quat. Sci. Rev.* **2020**, *239*, 106359. [CrossRef]
32. Xiao, X.; Yao, A.; Hillman, A.; Shen, J.; Haberle, S.G. Vegetation, climate and human impact since 20 ka in central Yunnan province based on high-resolution pollen and charcoal records from Dianchi, southwestern China. *Quat. Sci. Rev.* **2020**, *236*, 106297. [CrossRef]
33. Chen, X.; Wu, D.; Huang, X.; Lv, F.; Brenner, M.; Jin, H.; Chen, F. Vegetation response in subtropical southwest China to rapid climate change during the Younger Dryas. *Earth-Sci. Rev.* **2020**, *201*, 103080. [CrossRef]
34. Li, K.; Liao, M.; Ni, J. Vegetation response to climate change and human activity in southwestern China since the Last Glacial Maximum. *Palaeogeog. Palaeoclim. Palaeoecol.* **2024**, *636*, 111990. [CrossRef]

35. Sugita, S. Theory of quantitative reconstruction of vegetation I: Pollen from Large Sites REVEALS regional vegetation composition. *Holocene* **2007**, *17*, 229–241. [CrossRef]
36. Hellman, S.; Gaillard, M.; Broström, A.; Sugita, S. The REVEALS model, a new tool to estimate past regional plant abundance from pollen data in large lakes: Validation in southern Sweden. *J. Quat. Sci.* **2008**, *23*, 21–42. [CrossRef]
37. Li, B.; Zhang, W.; Fyfe, R.; Fan, B.; Wang, S.; Xu, Q.; Zhang, N.; Ding, G.; Yang, J.; Li, Y. High-resolution quantitative vegetation reconstruction in the North China Plain during the early-to-middle Holocene using the REVEALS model. *Catena* **2024**, *234*, 107577. [CrossRef]
38. Nanjing Institute of Geography and Limnology, Chinese Academy of Sciences. *Environments and Sediments of Fault Depression Lakes in Yunnan*; Science Press: Beijing, China, 1989. (In Chinese)
39. Nanjing Institute of Geography and Limnology, Chinese Academy of Sciences. *Lake Fuxian*; Ocean Press: Beijing, China, 1990. (In Chinese)
40. Yang, L.; Li, H. (Eds.) *Wetlands of Yunnan*; China Forestry Publishing House: Beijing, China, 2010. (In Chinese)
41. Wang, S.; Du, H. *Annals of Lakes in China*; Science Press: Beijing, China, 1998. (In Chinese)
42. Editorial Board of Vegetation Map of China, Chinese Academy of Sciences. *Vegetation Atlas of China*; Science Press: Beijing, China, 2001. (In Chinese)
43. Cheng, S.; Li, Y. Geomorphology of the Fuxian drainage basin and its structural implication. *J. Geomech.* **2010**, *16*, 383–391. (In Chinese)
44. Kong, W.; Wang, Y.; Xiang, L.; Wang, Z.; He, Z.; Yang, S. An analysis on the landscape pattern of the vegetation in Fuxian Lake basin in Yunnan. *J. Yunnan Univ.* **2012**, *34*, 468–475. (In Chinese)
45. Ai, J.; Wen, Q.; Tao, J. Study on forest vegetation and its value of soil and water conservation in Lake Fuxian Basin, Yunnan Province. *J. Anhui Agri. Sci.* **2010**, *38*, 11010–11012.
46. Faegri, K.; Iversen, J. *Textbook of Pollen Analysis*; Macmillan: New York, NY, USA, 1975.
47. Stockmarr, J. Tablets with spores used in absolute pollen analysis. *Pollen Spores* **1971**, *13*, 615–621.
48. Matthias, I.; Giesecke, T. Insights into pollen source area, transport and deposition from modern pollen accumulation rates in lake sediments. *Quat. Sci. Rev.* **2014**, *87*, 12–23. [CrossRef]
49. Grimm, E.C. TILIA and TILIA.GRAPH: PC Spreadsheet and Graphics Software for Pollen Data, Version 2.0.b.4. *INQUA Comm. Study Holocene Work.-Group Data Handl. Methods* **1990**, *4*, 5–7.
50. Grimm, E.C. CONISS: A FORTRAN 77 program for stratigraphically constrained cluster analysis by the method of incremental sum of squares. *Comput. Geosci.* **1987**, *13*, 13–35. [CrossRef]
51. Kassambara, A.; Mundt, F.; factoextra: Extract and Visualize the Results of Multivariate Data Analyses. R Package Version 1.0.7. 2020. Available online: https://CRAN.R-project.org/package=factoextra (accessed on 26 December 2023).
52. R Core Team. *R: A Language and Environment for Statistical Computing*; R Foundation for Statistical Computing: Vienna, Austria, 2023. Available online: https://www.R-project.org/ (accessed on 26 December 2023).
53. Wang, M.; Sun, Q.; Meng, H.; Huang, L.; Li, H.; Zhang, H.; Shen, C. Holocene vegetation dynamics revealed by a high-resolution pollen record from a large lake in central Yunnan, Southwest China. *Land* **2024**, *13*, 782. [CrossRef]
54. Theuerkauf, M.; Couwenberg, J.; Kuparinen, A.; Liebscher, V. A matter of dispersal: REVEALSinR introduces state-of-the art dispersal models to quantitative vegetation reconstruction. *Veg. Hist. Archaeobotany* **2016**, *25*, 541–553. [CrossRef]
55. Liu, Y.; Sun, H.; Zhou, X.; Duan, L.; Li, H.; Zhang, H. Paleoenvironmental significance of organic carbon isotope in lacustrine sediments in Lake Fuxian during the past 5 ka. *J. Lake Sci.* **2017**, *29*, 722–729. (In Chinese)
56. Reimer, P.J.; Austin, W.E.; Bard, E.; Bayliss, A.; Blackwell, P.G.; Ramsey, C.B.; Butzin, M.; Cheng, H.; Edwards, R.L.; Friedrich, M.; et al. The IntCal20 northern hemisphere radiocarbon age calibration curve (0–55 cal ka BP). *Radiocarbon* **2020**, *62*, 725–757. [CrossRef]
57. Sugita, S.; Parshall, T.; Calcote, R.; Walker, K. Testing the landscape reconstruction algorithm for spatially explicit reconstruction of vegetation in northern Michigan and Wisconsin. *Quat. Res.* **2010**, *74*, 289–300. [CrossRef]
58. Serge, M.A.; Mazier, F.; Fyfe, R.; Gaillard, M.-J.; Klein, T.; Lagnoux, A.; Galop, D.; Githumbi, E.; Mindrescu, M.; Nielsen, A.B.; et al. Testing the effect of relative pollen productivity on the REVEALS model: A validated reconstruction of Europe-wide Holocene vegetation. *Land* **2023**, *12*, 986. [CrossRef]
59. Yunnan Forest Writing Committee. *Forests of Yunnan*; Yunnan Science and Technology Press & China Forestry Publishing House: Kunming, China, 1986. (In Chinese)
60. Laskar, J.; Robutel, P.; Joutel, F.; Gastineau, M.; Correia, A.C.M.; Levrard, B. A long-term numerical solution for the insolation quantities of the Earth. *Astron. Astrophys.* **2004**, *428*, 261–285. [CrossRef]
61. Zhang, X.; Zheng, Z.; Huang, K.; Cheng, J.; Cheddadi, R.; Zhao, Y.; Liang, C.; Yang, X.; Wan, Q.; Tang, Y.; et al. Quantification of Asian monsoon variability from 68 ka BP through pollen-based climate reconstruction. *Sci. Bull.* **2023**, *68*, 713–726. [CrossRef]
62. Cheng, H.; Edwards, R.L.; Sinha, A.; Spöt, C.; Yi, L.; Chen, S.; Kelly, M.; Kathayat, G.; Wang, X.; Li, X.; et al. The Asian monsoon over the past 640,000 years and ice age terminations. *Nature* **2016**, *534*, 640–646. [CrossRef]
63. Dutt, S.; Gupta, A.K.; Clemens, S.C.; Cheng, H.; Singh, R.K.; Kathayat, G.; Edwards, R.L. Abrupt changes in Indian summer monsoon strength during 33,800 to 5500 years B.P. *Geophys. Res. Lett.* **2015**, *42*, 5526–5532. [CrossRef]
64. Mohtadi, M.; Prange, M.; Oppo, D.W.; Pol-Holz, R.D.P.; Merkel, U.; Zhang, X.; Steinke, S.; Lückge, A. North Atlantic forcing of tropical Indian Ocean climate. *Nature* **2014**, *509*, 76–80. [CrossRef]

65. Grootes, P.M.; Stuiver, M. Oxygen 18/16 variability in Greenland snow and ice with 10^{-3}- to 10^{5}-year time resolution. *J. Geophys. Res.* **1997**, *102*, 26455–26470. [CrossRef]
66. Wang, Q.; Yang, X.; Anderson, N.J.; Zhang, E.; Li, Y. Diatom response to climate forcing of a deep, alpine lake (Lugu Hu, Yunnan, SW China) during the Last Glacial Maximum and its implications for understanding regional monsoon variability. *Quat. Sci. Rev.* **2014**, *86*, 1–12. [CrossRef]
67. Xiao, X.; Zhao, Y.; Chi, C.; Zheng, Z.; Ma, C.; Liang, C.; Mao, L.; Hillman, A. Quantitative pollen-based paleoclimate reconstructions for the past 18.5 ka in southwestern Yunnan Province, China. *Glob. Planet. Chang.* **2023**, *230*, 104288. [CrossRef]
68. Xiao, X.; Haberle, S.G.; Shen, J.; Xue, B.; Burrows, M.; Wang, S. Postglacial fire history and interactions with vegetation and climate in southwestern Yunnan Province of China. *Clim. Past* **2017**, *13*, 613–627. [CrossRef]
69. Li, Y.; Chen, X.; Xiao, X.; Zhang, H.; Xue, B.; Shen, J.; Zhang, E. Diatom-based inference of Asian monsoon precipitation from a volcanic lake in southwest China for the last 18.5 ka. *Quat. Sci. Rev.* **2018**, *182*, 109–120. [CrossRef]
70. Zong, Y.; Lloyd, J.M.; Leng, M.J.; Yim, W.W.-S.; Huang, G. Reconstruction of Holocene monsoon history from the Pearl River Estuary, southern China, using diatoms and carbon isotope ratios. *Holocene* **2006**, *16*, 251–263. [CrossRef]
71. Wang, M.; Meng, H.; Huang, L.; Sun, Q.; Zhang, H.; Shen, C. Vegetation succession and forest fires over the past 13 000 years in the catchment of Yangzonghai Lake, Yunnan. *Quat. Sci.* **2020**, *40*, 175–189. (In Chinese)
72. Fan, Y. Histories of Vegetation, Climate and Forest Fire over the Last 15,400 Years in the Yilong Lake Catchment of Southern Yunnan. Master's Thesis, Yunnan Normal University, Kunming, China, 2021.
73. Wu, J.; Shen, C.; Yang, H.; Shi, Q.; Xie, S. Holocene temperature variability in China. *Quat. Sci. Rev.* **2023**, *312*, 107184. [CrossRef]
74. Liu, G.; Li, X.; Chiang, H.C.; Chawchai, S.; He, S.; Lu, Y.; Aung, L.T.; Maung, P.M.; Tun, W.N.; Oo, K.M.; et al. On the glacial-interglacial variability of the Asian monsoon in speleothem $\delta^{18}O$ records. *Sci. Adv.* **2020**, *6*, eaay8189. [CrossRef]
75. Cai, Y.; Zhang, H.; Cheng, H.; An, Z.; Lawrence, E.R.; Wang, X.; Tan, L.; Liang, F.; Wang, J.; Kelly, M. The Holocene Indian monsoon variability over the southern Tibetan Plateau and its teleconnections. *Earth Planet. Sci. Lett.* **2012**, *335–336*, 135–144. [CrossRef]
76. Hillman, A.L.; Abbott, M.B.; Finkenbinder, M.S.; Yu, J. An 8600 year lacustrine record of summer monsoon variability from Yunnan, China. *Quat. Sci. Rev.* **2017**, *174*, 120–132. [CrossRef]
77. Wang, X.; Huang, X.; Sachse, D. Two-phase hydrological changes during the mid-to late Holocene transition in Southwest China. *Quat. Sci. Rev.* **2023**, *322*, 108432. [CrossRef]
78. Bond, G.; Broecker, W.; Johnsen, S.; McManus, J.; Labeyrie, L.; Jouzel, J.; Bonani, G. Correlations between climate records from North Atlantic sediments and Greenland ice. *Nature* **1993**, *365*, 143–147. [CrossRef]
79. Wang, Y.; Cheng, H.; Edwards, R.L.; He, Y.; Kong, X.; An, Z.; Wu, J.; Kelly, M.J.; Dykoski, C.A.; Li, X. The Holocene Asian mon-soon: Links to solar changes and North Atlantic climate. *Science* **2005**, *308*, 854–857. [CrossRef]
80. Gupta, A.K.; Anderson, D.M.; Overpeck, J.T. Abrupt changes in the Asian southwest monsoon during the Holocene and their links to the North Atlantic Ocean. *Nature* **2003**, *421*, 354–357. [CrossRef]
81. Shen, C. Millennial-Scale Variations and Centennial-Scale Events in the Southwest Aian Monsoon: Pollen Evidence from Tibet. Ph.D. Thesis, Louisiana State University, Baton Rouge, LA, USA, 2003.
82. Duan, F.; Zhang, Z.; Liu, D.; Chen, J.; Shao, Q.; Wang, Y. Stalagmite-based long-term and multi-centennial hydroclimatic variations in southwestern China during the Holocene and relations to global climate change. *Quat. Sci. Rev.* **2023**, *319*, 108327. [CrossRef]
83. Hillman, A.L.; Yu, J.; Abbott, M.B.; Cooke, C.A.; Bain, D.J.; Steinman, B.A. Rapid environmental change during dynastic transitions in Yunnan Province, China. *Quat. Sci. Rev.* **2014**, *98*, 24–32. [CrossRef]
84. Hillman, A.L.; O'Quinn, R.F.; Abbott, M.B.; Bain, D.J. A Holocene history of the Indian monsoon from Qilu Lake, southwestern China. *Quat. Sci. Rev.* **2020**, *227*, 106051. [CrossRef]
85. Yao, A.; Jiang, Z.; Chen, X.; Liang, Y. Bronze Age wetland/scapes: Complex political formations in the humid subtropics of southwest China, 900–100 BC. *J. Anthropol. Archaeol.* **2015**, *40*, 213–229. [CrossRef]
86. Dal Martello, R.; Li, X.; Fuller, D. Two-season agriculture and irrigated rice during the Dian: Radiocarbon dates and archaeobotanical remains from Dayingzhuang, Yunnan, Southwest China. *Archaeol. Anthropol. Sci.* **2021**, *13*, 62. [CrossRef]
87. Yao, A.; Jiang, Z. Rediscovering the settlement system of the 'Dian' kingdom, in Bronze Age southern China. *Antiquity* **2012**, *86*, 353–367. [CrossRef]
88. Dong, X.; Wu, Y. *Vicissitudes of Lake Dianchi: Millennium Environmental History Perspective*; Intellectual Property Publishing House: Beijing, China, 2013. (In Chinese)
89. He, Y.; Xia, G. *The General History of Yunnan*; China Social Sciences Press: Beijing, China, 2011. (In Chinese)
90. Fitzgerald, C.D. *The Southern Expansion of the Chinese People*; Australian National University Press: Canberra, Australia, 1972.